Optimization of the Porosity of Refractory Materials to Achieve the Desired Mechanical Properties

by

Ayan Pal

Examination Roll No: M4MAT24004

Registration No: 163732 of 2022-2023

A Thesis Submitted in the Partial Fulfilment of the Requirements for the Degree of

Master of Technology in Material Engineering

Department of Metallurgical & Material Engineering

Faculty of Engineering & Technology (FET)

Jadavpur University

Kolkata-700032

India

2024

CERTIFICATE

This is to certify that the thesis entitled "**Optimization of the porosity of refractory materials to achieve the desired mechanical properties**" submitted by **Mr. Ayan Pal**, for the award of degree of Master of Technology in Material Engineering from the Department of Metallurgical and Material Engineering of Jadavpur University is absolutely based on his own work under the supervision of **Dr. Rajib Dey** and **Dr. Gopes Chandra Das** and that neither this thesis nor any part of the same has been submitted for any degree/diploma or any other academic award anywhere before.

……	**……**
Supervisor	**Supervisor**
Dr. Rajib Dey	**Dr. Gopes Chandra Das**
Professor	**Ex- Professor**
Metallurgical and Material Engineering Department	**Metallurgical and Material Engineering Department**
Jadavpur University	**Jadavpur University**
Kolkata-700032	**Kolkata-700032**

……	**……**
Head of The Department	**DEAN**
Dr. Sathi Banerjee	**Prof. Dipak Laha**
Metallurgical and Material Engineering Department	**Faculty of Engineering and Technology (FET)**
Jadavpur University	**Jadavpur University**
Kolkata-700032	**Kolkata-700032**

STATEMENT OF ORIGINALITY

I, Ayan Pal, do hereby declare that this thesis entitled "**Optimization of the porosity of refractory materials to achieve the desired mechanical properties**" contains literature survey and original research work done by the undersigned candidate as part of Master of Technology degree in Material Engineering during the academic session 2022-2024.

All information in this thesis have been obtained and presented in accordance with existing academic rules and ethical conduct. I declare that, as required by these rules and conduct, I have fully cited and referred all materials and results that are not original to this work.

Name: Ayan Pal
Class Roll No: 002211303004
Registration No: 163732 of 2022-2023
Signature of Candidate:
Date:

CERTIFICATE OF APPROVAL

This is to certify that the thesis entitled "**Optimization of the porosity of refractory materials to achieve the desired mechanical properties**" is hereby approved by the committee of final examination for evaluation of the thesis as a creditable study of an engineering subject submitted by **Mr. Ayan Pal** (Registration No: 163732 of 2022-2023) in a manner satisfactory to warrant its acceptance as a prerequisite to the degree of Master of Technology in Material Engineering. It is understood that by this approval, the undersigned do not necessarily endorse or approve any statement made, opinion expressed or conclusion drawn therein, but approve the thesis only for the purpose for which it is submitted.

Committee of final examination for evaluation of thesis-

…….. ……

……... ……

Dedicated

to

My Family

Acknowledgment

I would like to take this opportunity to express my gratitude towards every individual who has remained by my side throughout this entire journey. My entire M. Tech journey has been a rollercoaster ride of learning, happiness, struggle, and frustration. Without the constant support and guidance of all these people, this journey would have not been possible.

Firstly, I would like to acknowledge the contribution of Dr. Rajib Dey, Professor, Metallurgical and Material Engineering Department, Jadavpur University, Kolkata who has not only been my technical mentor but also been my friend, philosopher, and guide. During my toughest of times, his motivation and guidance have acted as a blessing

I would also like to express my respect and admiration towards ex-professor Dr. Gopes Chandra Das of the Metallurgical and Material Engineering Department, Jadavpur University, Kolkata for his constant guidance and support throughout the work. His academic wisdom has been a boon for me in my research work.

I also owe my success to all the professors and lab technicians of this department without whom my journey would have been incomplete.

My special thanks to all my lab seniors Sourav Adhikary, Santosh Khan, for their constant support throughout my journey. In the toughest of my times, they acted as pillars of support and the brotherhood I developed with them will remain forever even beyond my research journey.

'True friends are like diamonds, precious and rare' and I have been fortunate enough to get a few of them in my life. My school friends as well as my college friends have remained by my side throughout the journey and from the bottom of my heart, I thank all of them for supporting me in every way possible

I am forever indebted to my parents and family members for bearing with all my frustrations throughout my journey. My decision to leave a job midway and continue my academic career appeared as a shock for everybody except my parents who have never forced me to set aside my aspirations and supported me in every way possible. Today on the verge of completing my MTech, I dedicate my success to them.

Ayan Pal

List of Contents

List of Figures

List of Tables

CHAPTER – 1

INTRODUCTION

Background:

Refractories are the type of ceramic materials that can endure high temperatures and loads. They serve as the "backbone of the industry" since they support the manufacturing of all commodities that involve high temperatures like steel, cement, petrochemicals, glass, etc. Refractories are defined in the ASTM C71 specification as nonmetallic materials possessing the chemical and physical properties that make them suitable for systems above 1000°F (811°K or 538°C) though today refractories are used for environments exceeding 1500ºC [1]. The iron and steel industry accounts for around 70% of the consumption of refractories. Some other major industries include cement (7%), glass (5%), chemicals (4%) etc. [2].

Since the application areas of refractories involve high temperatures, they must possess good mechanical properties especially strength, at elevated temperatures. Apart from mechanical properties other important properties are thermal conductivity, corrosion resistance, etc. Refractory materials always consist of voids. The porosity contributes a very important role in determining the properties of refractory materials. The presence of pores leads to poor mechanical strength and corrosion resistance. Again, porosity is desirable for good insulating properties of refractories. In this case, an attempt has been made to study some of the major factors influencing the properties of fire clay refractories and optimization of the affecting parameters through mathematical modeling [3].

Present Scenario of Refractory Industry:

Refractories play a significant role in the operations of almost every industry, some noteworthy among them are iron & steel, cement, glass, petrochemicals, etc. The cost of refractory products contributes less than 3% of the total cost of manufactured goods, according to the World Refractory Association. However optimal application and design of the refractory products can reduce the operational cost of the industries by up to 20%. In terms of consumption, the refractory market is split into iron & steel, cement, glass, and others. Among all of them iron & steel industry captures the highest proportion of the global refractory market due to its widespread usage in nearly all furnaces and vessels used in the production of steel [4]. Additionally, the frequent replacement of the refractory linings during various stages of steel production also contributes to high refractory consumption from the iron & steel industry. Alumina Zirconia Silica (AZS) is the major structural material used in glass furnaces primarily due to its non-contamination with molten glass and high corrosion resistance. The growth in the glass industry due to the transition from plastic towards more sustainable glass leads to a surge in demand for refractories. In the cement

industry, refractory bricks are used in rotary kilns. Other industries that use refractory materials include petrochemical, electric power, machinery, and military sectors. The steel industry being the biggest consumer of refractory products the overall refractory consumption depends on the steel production of the country. The production of crude steel in India has risen from 109.25 MT in 2018 to 124.72 MT in 2022. On a yearly basis, crude steel production has increased by 5.5% from 2021 to 2022 [5]. The government of India in its Union Budget for FY 2022-23 has emphasized the growth of the infrastructure sector which includes roads, logistics, public transport, commercial real estate, etc. This growth in infrastructure provides an exponential growth opportunity for India's refractory industry supported by the Government's initiative of 'Atmanirbhar Bharat'. Moreover, India's Steel Policy estimates a steel production of 300 MT by 2030. The cement sector is anticipated to develop by 12%, compared to a historical CAGR of 6%. This indicates that the refractory business has a large gap that needs to be filled. The revival of the automobile industry, particularly with the growth of electric vehicles (EV) has also created a strong momentum for vehicle manufacturing materials like steel, iron, and glass which is expected to further expand the refractory markets.

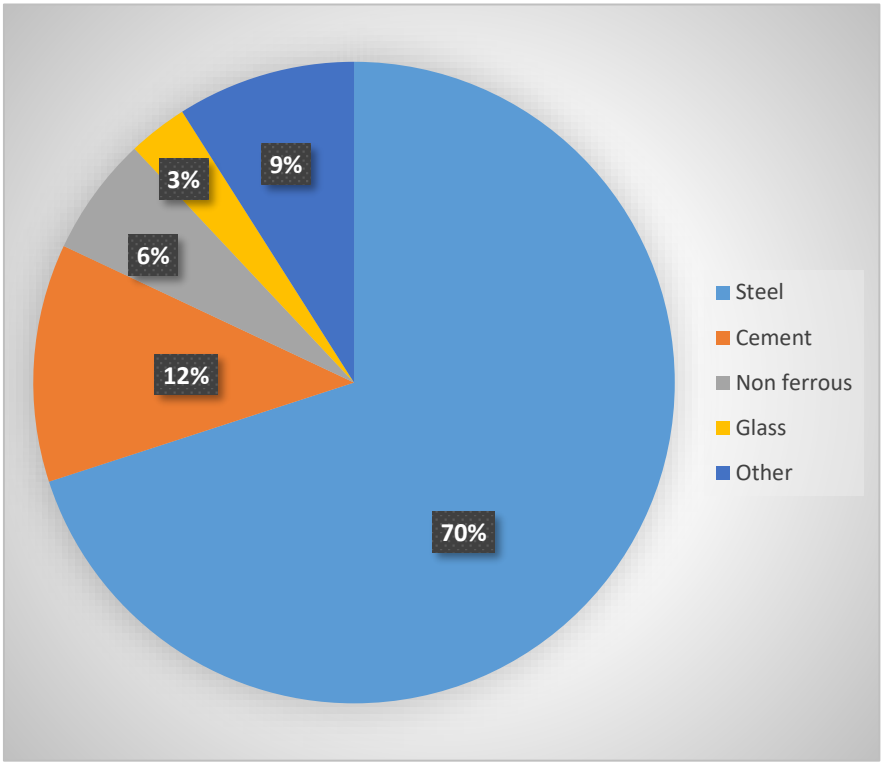

Fig 1. Industry-wise application of refractory materials

Classification of Refractories:

Refractories are frequently categorized according to their chemical behavior as acidic, basic, and neutral.

- **Acidic Refractories:** They are relatively stable in acidic environments but unstable in basic conditions. They mainly consist of silica as the major component. They form low melting silicate phases in any basic environments at high temperatures and hence are avoided. The applications of these refractories occur mainly in acidic environments such as glass tank furnaces, coke oven batteries, etc. Some examples of acidic refractories include Silica, Fireclay, etc [1].
- **Basic Refractories:** They are relatively stable in basic environments but unstable in acidic environments. They are extensively used in steel, non-ferrous, and cement industries. Some examples of basic refractories include Magnesia, Doloma, etc.
- **Neutral Refractories:** They are chemically inert in both acidic and basic environments. However, at high temperatures, these refractories develop some chemical affinity towards a particular environment (acidic or basic). Some examples of neutral refractories include Graphite, Alumina, etc. Among all neutral refractories, Graphite is the most inert. Alumina is stable at low temperatures but it becomes slightly acidic at higher temperatures.

Apart from chemical nature, the other parameters based on which refractories are classified are physical form, heat duty, porosity, etc.

- Based on physical forms the refractories are classified as shaped and unshaped.
- Based on the heat duty (application temperature) the refractories are classified as heavy, medium, and low.
- According to porosity the refractories are classified as dense and insulating.

Properties of Refractories: Refractories are materials that can withstand heat, and corrosion and possess high mechanical strength and thermal resistance. Different compositions of the refractories are adjusted to optimize the refractory properties for their applications in different environments. The different properties of refractories include physical, mechanical, thermal, etc. The main physical properties of the refractories include apparent porosity, bulk density, etc.

The porosity distribution in a refractory control its properties and application areas, hence it is very important to focus on the porosity of a refractory. The surface porosity (also denoted as apparent porosity) is defined as the ratio of the volume of surface pores to that of the total volume of the sample. Since refractories are mostly in contact with molten metal and slag, a refractory with low apparent porosity is desirable. The properties of refractories which are influenced by apparent porosity are given below:

- Thermal Conductivity: Higher apparent porosity leads to the presence of several voids in the material and since the voids are filled with air (which acts as an insulator) the thermal conductivity of the refractory decreases with an increase in porosity [6].
- Mechanical Properties: High porosity values lower the mechanical properties (CCS and MOR) of the refractories [7].
- Corrosion Resistance: Slag or penetration of any corrosive liquid is directly proportional to the number of pores present in the refractory surface thus a refractory with lower porosity will have high corrosion resistance.

The mechanical properties denote the action of refractories under mechanical forces in the application areas and thus are extremely crucial. The common mechanical properties of refractories include; Cold Crushing Strength (CCS) and Modulus of Rupture (MOR).

Cold Crushing Strength (CCS): This property is used to measure the compressive strength of refractories at room temperature and provide an idea regarding the load bearing capacity of refractory. It measures the bond strength of refractory material under compression and thus indirectly controls the performance of refractory. Higher densification (meaning lower apparent porosity) leads to higher CCS values, The CCS is represented by the equation:

$$\mathbf{CCS} = \frac{\mathbf{P}}{\mathbf{A}}$$

Where P = Compressive breaking load applied to the refractory material

A = Load application area

Modulus of Rupture (MOR): This property denoted the deformation resistance of a brittle material under bending stress. When performed at room temperature the property is known as Cold Modulus of Rupture (CMOR). The factors affecting the CMOR or Flexural Strength are the rate of loading; sample size and apparent porosity. The Flexural Strength is represented by the following equations as per the geometry of the sample:

$$\boldsymbol{Flexural\ Strength} = \frac{\mathbf{3PL}}{\mathbf{2bd^2}}$$ for the 3-point test of a rectangular specimen

$$= \frac{\mathbf{PL}}{\boldsymbol{\pi r^3}}$$ for the 3-point test of a round specimen

$$= \frac{\mathbf{3Pa}}{\mathbf{2bd^2}}$$ for the 4-point test of a rectangular specimen

$$= \frac{\mathbf{2Pa}}{\boldsymbol{\pi r^3}}$$ for the 4-point test of a round specimen

where P = bending load at breaking (rupturing) point, L = distance between the supporting points, b = breadth of the rectangular bar sample, d = depth (height) of the rectangular bar sample, r = radius of cylindrical rod sample, and a = (distance between the supporting points − distance between the loading points)

Thus, we observe that the mechanical properties of refractories are indirectly dependent on the apparent porosity of the material and thus minimization of porosity can ultimately lead to improvement in mechanical properties of the refractory.

Fireclay Refractories: Fireclay refractories are generally hydrated aluminosilicates containing around 25–45 wt. % of alumina and the rest of silica as the major component. It is mainly used for low-temperature areas and is inferior when compared to silica and magnesia refractories in terms of their chemical resistance. The main raw material of the fireclay refractory is naturally available fireclay. Since the fireclay refractories consist of aluminosilicate phases, from the Al_2O_3- SiO_2 phase diagram it is evident that 1587ºC is the eutectic temperature for pure fireclay. In the phase diagram, the region having 25-45 wt. % of alumina represents the fireclay refractories [8].

In manufacturing fireclay refractories along with the raw fireclay, some fractions of grog are also added. Grog is mainly used as an anti-shrinkage material to prevent high shrinkage and cracking of the refractories. Also, the addition of grog into the refractory composition lowers the porosity and increases the strength of the fireclay refractories [9].

The firing step of the fireclay refractories is a bit cautious due to the structural changes; moisture loss and volatile matter evolution associated with it and requires a relatively long firing schedule. The application areas of fireclay refractories include blast furnace stack, aluminum baking furnace, hot blast stove, preheating zones of rotary kilns used in cement industries, etc.

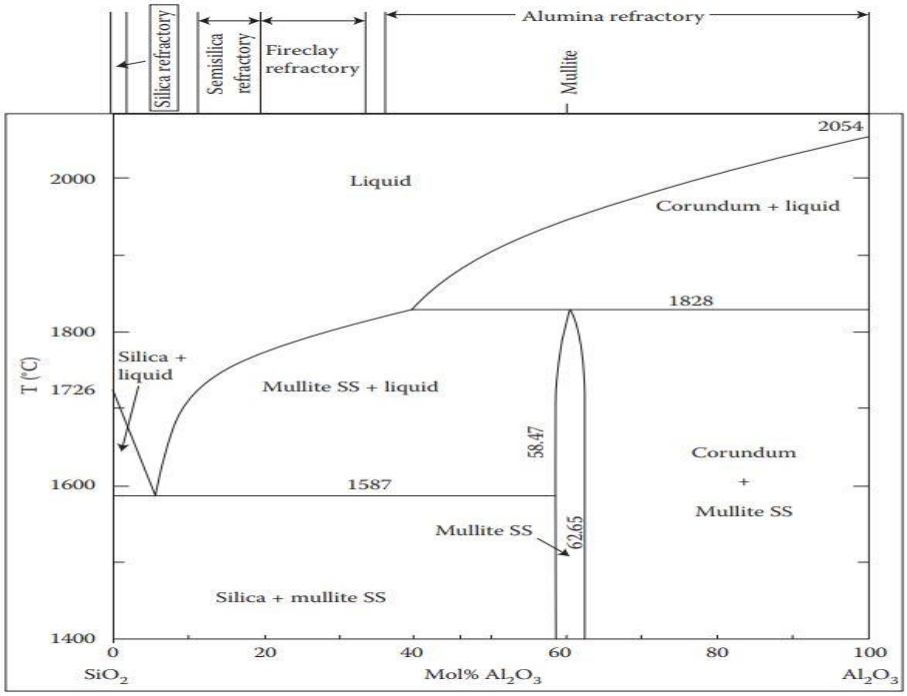

Fig 2. Al_2O_3-SiO_2 phase diagram

Optimization Techniques:

Refractories find application in nearly all heat-related industries, including the metallurgical, chemical, cement, glass, and petrochemical sectors. Refractory materials typically have a strong impact on the cost of the products. High-quality refractory at a reasonable cost is necessary since refractory costs increase the cost of production and thus optimization of the parameters influencing the mechanical properties of refractories is essential.

Stochastic optimization methods are often based on maximizing or minimizing an objective function that roughly corresponds to the system that has to be optimized. While several optimization techniques, such as response surface and mixture approaches, have been utilized in experiments with well-defined variables, the Taguchi optimization technique has been widely implemented in many research and is growing in popularity [10]. When a large number of interactions between experimental variables or components are anticipated, the Taguchi optimization technique plays a crucial role in reducing costs.

Dr. Genichi Taguchi developed the Taguchi method to investigate the effect of different parameters on the mean and variance of a process. Taguchi proposed an experimental design in which the process parameters and their appropriate levels are arranged using orthogonal arrays. This method involves system design, parameter design, and tolerance design for achieving the optimal condition. To analyze the results of orthogonal arrays and the contribution of influencing factors ANOVA (Analysis of Variance) is used [11].

In this work, the parameters influencing the mechanical properties of fireclay bricks are studied and the influence of the preferred 5 parameters (i.e., coarse size fraction, medium size fraction, fine size fraction, sintering temperature, and soaking time) on the mechanical properties have been optimized. Here the mechanical properties are directly linked to the apparent porosity of the material and hence apparent porosity has been chosen as the response variable in this experiment due to the ease of measurement. Since lower porosity leads to higher density and higher mechanical strength, the objective is to minimize the porosity [12].

CHAPTER – 2

LITERATURE REVIEW

Refractory materials: Refractories are ceramic materials which can resist high temperatures without any deformation. Refractories are the essential pre-requisite for any elevated temperature operation. They find significant applications in steel, cement, glass, chemical and metallurgical industries where they are used mainly as the inner linings of kilns, and furnaces. Today not only in the ferrous and nonferrous industries but also in advanced applications like nuclear reactors, missiles and modern rockets; refractory materials are used. Refractory materials typically have a distinctive effect on the cost and quality of the products and hence high-quality refractory material at minimum cost is desirable in all industries. Refractory materials mainly constitute one or more minerals as the refractory medium along with or without reinforcing additives. The cohesiveness of the two phases is ensured by a suitable binder which is also added in to the medium. A number of physical characteristics such as apparent porosity, bulk density, and strength at room temperature, must be taken into account when selecting a refractory for a certain application. Hence density and porosity are the mostly examined properties. The particle size distribution of the raw materials, pressing load, moisture content during loading, sintering temperature and sintering duration significantly affects the density, strength and porosity of the fired products. Apart from porosity and density, firing shrinkage is another significant property which needs to be addressed because high firing shrinkage can lead to cracking. The correlation of the properties with the production conditions through mathematical modelling is a unique aspect of this study [1].

Fireclay Refractories: Fireclay refractories belong to the alumina-silicate group of refractories having Al_2O_3content between 25-45% and remaining SiO_2 along with small contents of Fe_2O_3 (<5%) and TiO_2 (<2%) as impurities. The high temperature properties of these refractories depend largely on the Al_2O_3 content [13]. A higher percentage of Al_2O_3 will lead to an improvement in high temperature properties of fireclay refractories. Chemically they belong to the group of acidic refractories however their corrosion resistance in acidic environments is low compared to the silica refractories. In metallurgical industries fireclay refractories are used in the internal linings of hot metal and slag containing vessels like furnaces, ladles, kilns, reactors etc [14]. In non-metallurgical industries they are used in hydrogen reformers, cracking furnaces, coke calciner, lime kilns, utility boilers etc. The fireclay refractories contribute nearly 50-55% of the total production of refractories by volume. Depending upon their ability to withstand temperature before melting they are classified into i) Low duty ii) Intermediate duty iii) High duty and iv) Super duty

Raw Materials: The raw materials used in the production of refractories are mostly naturally occurring. The naturally available fireclay is the main raw material for fireclay refractories. Fireclays are sedimentary clays found in areas adjacent to coal mines. They can be further divided into two types according to their origin

(a) Underclays which are purer, softer and plastic and are found just below coal seam
(b) Shales which are harder and found on the top of coal seam

Fireclays are secondary in nature and hence acquires impurities during transportation. The hardness of fireclays varies according to their origin as underclays or shales and their specific gravity lies in the range 2.60-2.65 .

The fireclay as bedded deposits are mostly associated to coal measures from Tertiary and Gondwana periods. The significant deposits are found in the Jharia and Raniganj coalfields in West Bengal and Jharkhand, Korba coalfield in Chhattisgarh and NeyveliLignite field in Tamil Nadu. The fireclays which are not associated with the coal measures are found in Gujrat, Sundergarh-Belpahar areas of Orissa and Jabalpur areas of Madhya Pradesh [15].

Grog and its use in Fireclay refractories: Fireclay is a secondary clay consisting of very fine particles and hence using only raw fireclay will lead to huge shrinkage during drying and defects such as cracking, and warpage will arise during firing. Thus, along with raw clay, another material called grog is used in the fireclay refractory composition. Grog is a pre-calcined clay that is added to the mix to lower the firing shrinkage and improve the application stability [16]. For efficient compaction of the refractory body, the particles in the mixture are segregated into different fractions (coarse, medium, and fine). In this case, the grog is crushed into different size fractions and added into the mix and the raw fireclay is typically used as the finer size fraction. The grog content varies from one product to another and it is mainly used as an anti-shrinkage material to reduce the defects in the final product and improve the density and strength of the material [9].

Manufacturing Process of Fireclay refractories: The grog is crushed using a jaw crusher and roll crusher to obtain grog particles of different size fractions. These grog fractions along with raw fine clay and binder are mixed uniformly with a required amount of water (4-12%) and are pressed in a hydraulic press. The compaction pressure ranges between 50-80 MPa for fireclay refractories. The pressed products are then dried followed by the firing of the products. Firing is a critical step and is accompanied by different phase formations and shrinkage. The first stage of firing occurs at about 500°C which involves the elimination of both physically and chemically absorbed water. The second stage of firing which occurs up to 900°Cinvolves the decomposition of carbonates and sulfates. In the third stage of firing (till 1300°C) the metakaolin decomposes to form mullite and excess silica. At temperatures above 1300°C liquid formation occurs which enhances the sintering. The liquid phase fills the interparticle gaps and as a result, a dense and compact body is obtained. The over-firing of the refractories can lead to deformation due to excess liquid formation whereas under-firing can result in lower strength of the refractories. Thus, optimized firing is necessary to obtain the proper strength of the fireclay refractory products.

Application areas of Fireclay refractories: Due to its low cost, it is widely used in low-temperature areas. The acidic nature of the refractories restricts its application in basic environments. The major areas of application are given below:

- **Blast Furnace:** They are used in the upper stack of blast furnaces where the temperature ranges between 300°C to 800°C. The carbon-monoxide environment in this area requires fireclay refractories with max 1.5% Fe_2O_3 content.
- **Cement Rotary kiln:** They are used in the preheating and calcining zones of cement rotary kilns where the temperature varies from 300°C to 1100°C. The Al_2O_3 content varies between 25% and 45% depending on the application temperature.
- **Glass tank furnace:** They are used in the checker works of the regenerators of glass tank furnaces due to their high creep resistance and thermal shock resistance till 1300°C. High alumina content (40-45%) fireclay refractories are also used in regenerator walls and backup areas of the melting tank.
- **Baking furnace of aluminum industries:** Fireclay refractories with high grog content are used in the flue ducts of baking furnace. Fireclay refractories with alumina content 35%-40% are also used in the backup linings.

Factors affecting the properties of refractories:

Refractories are prepared from granular mass having different particle sizes and hence voids are present in between the particles even after firing. The voids present in the refractories are technically termed porosity. Porosity significantly influences the properties of refractories like mechanical strength, corrosion resistance, thermal conductivity, etc. and thus it is chosen as the response variable in our experiment. A low porosity leads to the formation of a dense refractory with high mechanical strength and thus reducing the porosity is the main aim of our study. The factors controlling the properties (and hence porosity) of the refractories are explained below:

1) **Particle size distribution:** Particle size distribution of the batch is crucial to achieve the highest possible bulk density and hence lower their apparent porosity. The grain size distribution is generally controlled using three different size fractions, coarse, medium, and fines in the batch composition through proper screening and crushing [17].

- For a single-component system, it has been observed that the packing depends on the shape and arrangement of the particles. Considering the simplest case with spheres, the different packing methods and their void percentage are shown in the table below:

Table 1. Different packing methods and void %

Packing types	**Void percentage (%)**
Cubical	47.64
Single stagger	39.55
Double stagger	30.20
Pyramidal	25.95
Tetrahedral	25.95

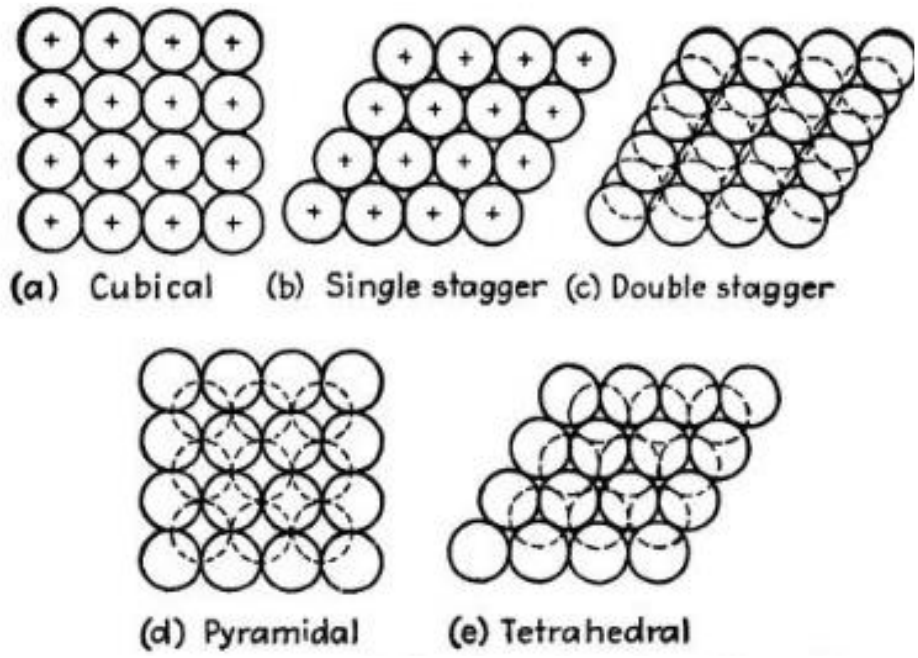

Fig 3. Different packing arrangements of particles

- Researchers have suggested different refractory batch compositions involving coarse, medium, and fine-size fractions. Some of them are mentioned below:

  In 1930 Hugill and Rees suggested a batch composition involving coarse, medium, and fine-size fractions in the ratio 45:10:45 respectively.

  In 1962 Gugel and Norton formulated a batch composition involving fireclay grog as coarse: medium: fine=50:10:40 which gave the densest mix having a minimum porosity of 23%.

  In 1970 Karisson and Spring suggested that for a three-component system involving irregularly shaped fireclay grog, the best proportion was 40:30:30.

  The experimental results have shown that 95.1% of theoretical density for a ternary system was achieved with diameter ratios 1:7:38:316 and volume compositions 6.1:10.2:23:60.7 %.

  Another study has revealed that a batch composition involving 40-45% coarse, 10-20% medium, and 40-45% fine fraction has achieved a maximum density close to the theoretical density. The different size fractions used in the study were, coarse (-4+30 BS mesh), medium (-30+80 BS mesh), and fine (-80 BS mesh).

  In the case of distribution of the particles into three size fractions viz, coarse, medium, and fine the packing is better compared to a single component system because the inter-particle voids between the coarse grains are filled up by the medium size grains and the voids between the coarse and medium grains are filled up by fine grains. The binder which is added into the batch composition further reduces the voids by forming a coating around all the grains.

2) **Sintering Temperature:** Sintering is the process of compacting a solid material by pressure or heat. The sintering temperature is generally lower than the melting point. Sintering generally lowers the porosity and increases the mechanical strength of the material. The sintering occurs at a temperature below the melting point (50-80% of the melting point) of the material. In case of ceramic materials sintering leads to the formation of strong ceramic bonds between the particles and thus reduces the porosity, and increases the bond area and mechanical strength. Apart from enhancing the mechanical properties sintering also increases the shrinkage of the material due to the following reasons:

- Ceramic materials try to reach the lowest energy state by eliminating the grain boundaries along the surfaces which are regions of high energy.
- The thermal energy gained by the ceramic material during sintering allows it to alter the size of grain boundaries and thus the porosity is also reduced [18].

The reduction of total surface free energy is the driving force of sintering. In the sintering process initially, neck growth occurs followed by mass transportation. The densification is the final stage of sintering [19]. During the initial stage of sintering a 5-10% reduction in pores occurs and this proceeds till the final stage where the maximum density close to the theoretical density is achieved. During the process of sintering neck formation occurs at the surface of contact between two particles with the gradual elimination of pores. The increase in pore size retards sintering. Similarly, entrapment of gas within the pores also prevents sintering. The variables affecting the sintering behavior in the presence of viscous liquid are the viscosity of the liquid, pore size, and surface tension of the liquid [20].

For fireclay refractories at temperatures above 1300°C the liquid phase formation occurs due to the presence of various impurities which enhances the sintering by filling the gaps between the particles. The liquid filling inside the pores may continue up to 1500°C which lead to the densification of the body accompanied with a shrinkage [21]. After firing the microstructure of fireclay refractories consist of mullite, cristobalite, glass, and residual quartz. High temperatures and longer soaking times lead to the disappearance of the cristobalite and residual quartz phase and only mullite and viscous glass is present in the microstructure of fireclay. The firing step is extremely crucial as over-firing may cause deformation of the fireclay refractories

due to excess liquid phase formation and under-firing will lead to lower mechanical strength. Thus, optimization of the sintering temperature and soaking period is very important to get a refractory with good mechanical properties.

3) **Pressing Load:** The molding pressure exerted during the shaping of the product helps the binder to fill the voids between the particles. Thus, molding pressure is inversely proportional to the apparent porosity of the product. Thus, higher pressing load leads to lower void spaces which can also be confirmed from the SEM images. The presence of excessive fine fraction and moisture content in the batch composition obstructs the removal of air during pressing. This entrapped air lowers the density in the pressed products. Thus, efficient de-airing of the entrapped air is essential to obtain dense products [22]. Again, over-pressing leads to cracks and lamination defects in the pressed products and thus should be avoided. To achieve uniform densification of the pressed products an applied pressure for an optimum period is necessary along with optimum size distribution and moisture content.

   In one such study involving alumina aggregates namely Tabular Alumina (TA), and White Fused Alumina (WFA) Schafföner.S; and et.al (2016) [23] found that a higher pressing load leads to a higher density. Between the above-mentioned alumina aggregates the density of WFA was found to be slightly higher compared to the TA sample for the same pressure. The Cold crushing strength (CCS) has also increased with increasing pressure [24]. TA sample has shown higher CCS value than WFA primarily due to better bonding during sintering. The inspection of the values of Young's modulus has also indicated a significant effect of the pressure and the nature of raw material on the values of Young's modulus.

   Refractoriness under Load (RUL) is another important property which indicates the temperature of deformation of refractory under a fixed load with increase in temperature. For the alumina aggregates Schafföner.S, and et.al (2016) found that samples with lower pressing load have resulted in a faster deformation with increase in temperature [23]. The softening temperature is slightly higher for WFA compared to TA however this difference becomes more significant for higher pressing loads [25].

4) **Percentage of water added:** Keeping the pressing load and firing temperature constant it has been observed that an increase in the water content leads to a decrease in bulk density of the product and a subsequent decrease in apparent porosity. Some other effects of the addition of water on the properties of the products are:

- Increase in water content leads to increase in firing shrinkage of the product
- A decrease in compressive strength has been observed with an increase in water content in the mixture due to the increase in porosity.

5) **Particle size distribution model and particle morphology:** A study using different alumina raw materials (TA, WFA and reactive alumina) has revealed that the green density, apparent density and linear shrinkage of the samples were independent on the particle size distribution model. The apparent density and apparent porosity values determined using Archimedes method has also not shown much difference for different particle size distribution models. On the contrary to the physical properties the mechanical properties were largely affected by the particle size distribution model. The significant lower CCS and Young's modulus values of the samples with modified Andreasen model were mainly attributed due to the higher proportion of large grain size fractions. The lower specific surface of the larger grains reduces their sintering effect and this leads to the lower strength of the larger grains compared to the fine particles [26]. Similar to the physical properties the thermomechanical properties were marginally affected by the particle size distribution model. The obvious difference between tabular alumina and white fused alumina during the RUL and CIC measurements indicates that the raw material was still the dominating factor for creep and softening at higher temperatures, while the particle size distribution model had only a negligible effect. Thus, apart from the mechanical properties the other properties were unaffected by the particle size distribution model [23].

   From the several alumina raw materials it has been observed that the white fused alumina samples had higher green density and lower sintering shrinkage whereas tabular alumina resulted in a lower apparent porosity. In general, the samples containing angular grains had a higher apparent porosity compared to the blocky samples and this difference was more pronounced in case of white fused alumina. The higher sphericity of the blocky particles compared to the angular ones has led to better packing resulting in higher apparent density and lower porosity [27]. Of the three different raw materials mentioned in the study the physical properties of WFA were significantly impacted by the particle size probably due to the higher fractions of sorted particles as can be concluded from the Young's modulus and CCS values [27]. The low Young's modulus values of the specimens containing angular particles were supported by Ishikawa; who observed lower Young's modulus in the case of low cement castable composed of thick rod-shaped particles [28]. It has been

observed that the WFA samples with blocky grains softened at a higher temperature compared to those of WFA containing angular particles. However, for tabular alumina, the exact reverse trend has been observed. The samples consisting of block-shaped particles have resulted in lower apparent porosity values which also reduces their creep strength.

Different optimization techniques:

Optimization leads to the improvement in the performance of the process or certain properties by determining the best combination of all the process controlling variables. This study involves the optimization of the apparent porosity (and hence mechanical strength) by finding specific design parameters that would provide the best possible response.

- **Fuller Distribution:** The Fuller curve method is mainly used in concrete technology for the improvement of mechanical properties through proper particle size distribution. The overall size distribution is termed as the grading of feed. For any given distribution there exists a set of ideal grading curves out of which the Fuller curve is one of them. This approach can be used to obtain refractory briquettes with optimum mechanical properties. The feed mix which is closest to the ideal Fuller curve provides the most compact product and hence maximum mechanical strength. This method involves two parameters: coefficient of uniformity (CU) and root mean square deviation (RMSD) which are used to measure the deviation of a mix from ideal Fuller curve. This approach has also been used to produce iron nuggets from raw iron ore of significant strength in one such study. The overall particle size distribution is termed as grading of the feed. The proper grading of the batch composition is essential for higher packing density of the feed. Grading is the relation between sieve size X_i(mm) and the total amount passing through the sieve Y_i. The ideal grading curve for highest packing density is obtained by plotting ideal percentage of material passing through a given set of standard sieves which is given by the equation:

  $P = [Dx/Dmax]^n * 100$ where $P = \%$ passing square aperture size Dx

  D_{max} = maximum particle size, (mm) $n = 0.5$ grading coefficient

  The CU for the 'Ideal' Fuller Curve is 36. The Coefficient of Uniformity is a good measure of deviation from its Fuller curve. Grading above Fuller curve implies the presence of more fines which leads to poor contact between the coarse particles whereas grading below the Fuller curve implies the presence of a lesser number of

fines to fill the voids between coarse particles. Thus, the best compaction of the refractory products with improved mechanical properties can be achieved using the concept of the Fuller curve. The two parameters RMSD and CU involved in Fuller's distribution will be discussed below:

Root Mean Square Deviation (RMSD) represents the deviation between the predicted values and experimental values for the feed samples. RMSD is the square root of summation of the squares of all the deviations on the ordinates (% passing through) of the standard distribution curve from the Fuller's curve on all the standard sieve sizes, divided by the number of sieves used and it is represented as;

$$\mathbf{RMSD} = \sqrt{\frac{\sum (\mathbf{X1} - \mathbf{X2})^{\mathbf{2}}}{\mathbf{n}}}$$

where X1 and X2 are the **% passing through** values of feed and ideal Fuller distribution respectively and n denotes the number of standard sieves involved in the analysis.

The Coefficient of Uniformity (CU) is another parameter involved in our study. CU is represented by the equation:

$$\mathbf{CU} = \mathbf{D60}/\mathbf{D10}$$

D60 and D10 represent the screen size for which 60% and 10% of the sample is smaller respectively. The values of D60 and D10 are calculated from the particle size distribution obtained by passing the feed through a set of standard sieves and noting down the percentage of feed retained in each sieve. The strength of the aggregate will be determined by the closeness of the actual size distribution curve to the ideal Fuller curve. The grading of the batch composition is understood by the comparison of the particle size distribution with the "Ideal Grading Curves". Fuller curve is one such ideal grading curve and the closeness of the actual size distribution curve to the Fuller curve determines the strength of the aggregate. The maximum value of CU is 36 and this is mainly observed for concrete aggregates [29] due to their large particle size but in our study the value of CU obtained will be much lower than the maximum value. From the different batch composition ratios, the one with the highest value of CU and lowest value of RMSD will have the better mechanical properties and will be chosen as the optimized batch composition for the study.

- **Response Surface Methodology (RSM):** Response Surface Methodology (RSM) is a data modeling tool that provides a relationship between independent variables and the system's response. This method was introduced by Box and Wilson in the year 1951 for designing experiments. This method involves fitting different mathematical methods to the experimental results generated from designed experiments and verifying the model by statistical techniques. The structure of the relationship between the response and the input parameters (independent variables) is generally unknown and thus determining the suitable approximation to the true relationship is the first step of RSM [12].

The different steps involved in the optimization using RSM approach are stated below:

1) Selection of input variables and the possible output variables (or responses)
2) Selection of experimental design strategy
3) Performing the experiments and getting the results
4) Fitting the obtained experimental data to a suitable model equation
5) Obtaining response graphs and verification of the model
6) Determination of the optimal set of experimental parameters
7) Representation of effects of input variables through 2D and 3D plots

Design of Experiment (DOE) is an important aspect of RSM. Design of Experiment involves a series of tests through which changes in the input variables are made and the effect on response variables is measured. Experimental design is effective in maximizing the information gained from a study while minimizing the data collection. Thus, the design of experiments is effective in getting definite conclusions from data by the use of minimum resources. The different types of Designed Experiments are:

- Full Factorial
- Box Behnken
- Taguchi modeling

The Taguchi method uses Orthogonal Arrays (OA) to help design of experiment. The Orthogonal Arrays provide minimum experiments required for optimization. The Signal to Noise ratios (S/N) is the logarithmic functions of the output which help in the prediction of the optimized results. Taguchi's method of design of experiment can easily be applied with limited statistical knowledge and thus it has gained significant popularity in the engineering and scientific community. Three different situations specified in this method are:

- Larger the better
- Smaller the better
- Minimum variation

In our study since the response is apparent porosity which needs to be minimized thus smaller better approach is considered. The different steps involved in Taguchi methodology are:

- Identification of main function
- Identification of noise factors, quality characteristics and testing conditions
- Identification of the objective function
- Identification of levels and controlling factors
- Selection of orthogonal array matrix experiment
- Performing the matrix experiment
- Analysis of data and prediction of optimum levels
- Conducting the verification experiment

In Taguchi method a statistical treatment called Analysis of Variance (ANOVA) is used for the analysis of the results of OA experiments and to determine the variation each influencing factor has contributed.

In our present study the response is apparent porosity which is optimized by Taguchi modelling and the chosen input variables are: coarse fraction, medium fraction, fine fraction, sintering temperature and soaking duration.

CHAPTER – 3

RESEARCH PROBLEM AND OBJECTIVE

Refractories are inorganic non-metallic substances, (mainly oxides) which can withstand high-temperature conditions by retaining their mechanical and chemical strength. Fireclay refractories belong to the group of aluminosilicate minerals used mainly in all high-temperature processes. The need for refractories for an industrially growing nation like India is enormous. Refractory materials typically have a significant impact on the cost of metal products and thus high-quality refractory products at **minimum cost** are desired [30].

Fireclay is one such popular refractory material that is extensively used due to its high melting temperatures. They also contain certain non-clay minerals such as quartz, feldspar, etc. The properties of any refractory depend on the particle size distribution of the minerals and their reaction at high temperatures. For choosing a refractory regarding a particular application, several physical properties such as apparent porosity, room temperature strength, etc. must be considered. The porosity, mechanical strength, and density of fired products are affected by several factors like particle size distribution of the materials, moisture content, molding pressure, firing temperature, firing duration, furnace atmosphere, etc. The stochastic optimization technique involves the minimization or maximization of the objective function. Several optimization methods like the response surface and mixture methods with well-defined variables have been applied in experimentation. Out of different response surface methods Taguchi method has gained more popularity. This method is instrumental in cost saving especially where a larger number of interactions is expected between the variables and factors [3].

The influence of different factors on the strength of fireclay refractories is the main objective of this study. The innovative part of this study is the correlation of the mechanical properties of the fireclay refractories with the production conditions through mathematical modeling. Additionally, the process conditions will also be optimized using the Taguchi method of response surface methodology to get the optimized response (which is the minimum apparent porosity in this case). This optimization will help to get the set of processing variables that will lead to the minimum apparent porosity of the fireclay samples and thus through this method the properties of the refractory bricks can be improved to a certain extent along with necessary cost minimization [11].

CHAPTER – 4
METHODOLOGY

The present chapter explains the overall methodology (in a step-by-step manner) which is involved in achieving the objective of the experiment. The steps are mentioned below

- The phases present in the collected fireclay grog will be characterized by XRD analysis. The composition of the grog will be studied by XRF analysis.
- The collected fireclay grog will be crushed using a jaw crusher and the crushed grog particles will be segregated into different-size fractions using BSS standard sieves with a vibrating sieve shaker. The particles will be divided into three different size fractions: coarse, medium, and fine [31].
- The coarse size fraction will consist of particles from-4mm to +0.5mm, medium size fraction will consist of particles from -0.5mm to +0.18mm and below 0.18mm the particles will represent fine size fraction.
- The three different size fractions mentioned above will be obtained using BSS sieves of -4+30, -30+80, and -80 for coarse, medium, and fine respectively.
- Initially a batch composition of (40-45) wt. % coarse, (10-20) wt. % medium and (40-45) wt. % fine will be taken. The particles of different size fractions will be homogeneously mixed along with clay or molasses (as binders) and water. The mixture will then be pressed using a hydraulic press to obtain a cylindrical specimen of specific dimensions. The obtained green specimen will be dried at 110^0C and will then be sintered at temperature $(1250\text{-}1400)^0$ C. Two cylindrical specimens, (one using clay as a binder and another using molasses as a binder) will be obtained using the same method to observe the stability of the specimens under their weight [32].
- Then different batch compositions will be prepared by varying the coarse, medium, and fine ratios, and then following the same procedure as above different cylindrical fired specimens can be prepared.
- Apart from particle size, the other varying parameters will be sintering temperature (1250^0C, 1350^0C, 1450^0C), soaking time, etc. In this way, by varying the different parameters several fired cylindrical specimens will be prepared.
- Then the different properties such as, apparent porosity (AP), bulk density (BD), volume shrinkage etc. will be determined for each of the samples using standard procedures and the data will be recorded in tabular form for further analysis.
- The most compact mixture of the raw material (in accordance to the ratio of coarse, medium and fine particles) will be optimized by Fuller distribution method.
- The effect of the controlling parameters on the properties of fireclay refractories will be optimized through Taguchi method by performing a definite set of experiments.

- The optimization will be verified by performing the experiment with the set of optimized parameters.
- The characterization of the fired sample prepared under optimized conditions will be performed using XRD and SEM analysis for microstructural study.

CHAPTER -5

INSTRUMENTS AND APPARATUS

This chapter involves the various equipment that has been used in this study for different purposes such as size reduction, sample preparation, characterization, etc. The presence of proper standardized equipment is extremely vital for getting the best experimental results in any study. The list of the different instruments/equipment used in our study are listed below:

- **Jaw Crusher:** It is mainly used for reducing the fireclay grog lumps into smaller ones. A jaw crusher consists of a fixed and moveable jaw and the crushing occurs in between the two jaws. The fixed jaw (also known as anvil jaw) remains vertical while the moveable jaw remains at an angle of 20^0 to 30^0 with the fixed jaw and reciprocates horizontally. The lumps trapped between the jaws experience a significant compressive force due to the eccentric movement of the moveable or swinging jaw. The large lumps are first broken into small sizes and are re-crushed and after sufficient reduction, they are discharged through the bottom of the machine. The opening and closing rates of the jaws range between 250 to 400 times per minute. The adjustable jaw gap and the tooth shape for the crushing plates influence the final output size of the grains.

Fig 4. Jaw crusher

- **Roll Crusher:** The output of the jaw crusher contains a relatively small amount of fine particles and hence the output of the jaw crusher is generally used as the input feed for the roll crusher. A roll crusher consists of two metal rolls that rotate in opposite directions and the feed particles trapped between the two rolls are reduced into small fragments through the compressive action. The feed size (or input size) ranges from 12-75 mm and the product size (or output size) ranges between 12mm to 1mm. The final output size depends on the gap between the two metal rolls. The reduction ratio for roll crusher

Fig 5. Roll Crusher

is generally 3 or 4 to 1; which suggests that the maximum particle diameter of the product is 1/3rd or 1/4th that of the feed. The product size is adjusted by a hydraulic mechanism operating through a torsion bar.

- **Disc Pulverizer:** It is mainly used for generating fine particles. They consist of two roughened cast iron plates of which one is stationary and the other is rotating. The type and spacing between the plates determine the output size and fineness of the feed. These are mainly used for grinding the coarse particles into fine ones.

Fig 6. Disc Pulverizer

- **Sieve shaker:** Sieving involves the process of separation of fine particles from coarse ones by passing them through a series of sieves having different openings. In a sieve shaker, the set of BSS standard sieves are arranged with the coarser one at the top and the finer one at the bottom, and with an increase in sieve number the fineness increases. The entire setup consists of a platform that is attached to the lower end of two supporting rods, a sieve holder, a retaining ring, and nuts on vertical support rods to hold the series of sieves together. In our study particles of size -4mm to +0.5mm (sieve no. 4-30), -0.5mm to +0.18mm (sieve no. 30-80), and below 0.18mm (sieve no. -80) are screened for coarse, medium and fine fractions respectively.

Fig 7. Sieve Shaker

- **High Precision Weighing Balance:** Proper and accurate weighing of the materials play a key role in the experimental work and for this reason a high precision weighing balance has been used in our study. The maximum capacity of the balance is 1000g. It consists of a measuring pan situated in the middle of the weighing balance and the balance is surrounded by a transparent covering to prevent the errors and fluctuations in readings due to dust and air. In our study weighing balance has been repeatedly used during sample preparation and apparent porosity measurement.

Fig 8. Weighing Balance

- **X-Ray Diffractometer (XRD):** The X-ray diffraction method is mainly used for the identification of unknown crystalline samples. In this study, the different phases present in raw fireclay and the sintered fireclay samples have been characterized by XRD. This characterization involves the principle of constructive interference of monochromatic X-rays and a crystalline sample. The X-rays generated by the cathode tube are filtered to obtain the monochromatic rays and are then directed towards the sample to obtain constructive interference according to Bragg's law ($n\lambda=2d\sin\theta$). Copper is commonly used as a target material for single-crystal diffraction. The orientation of the X-ray diffractometer allows the sample to rotate at an angle θ in the path of the parallel X-rays. A detector present collects the diffracted X-rays on the other side and the goniometer maintains the rotation of the sample. The data collected from XRD are then matched with the database using JCPDS to determine the exact phases present in the raw fireclay and sintered fireclay samples.

Fig 9. X-Ray Diffractometer

- **Scanning Electron Microscope (SEM):** In this study SEM has been used to observe the change in morphology of the fireclay samples after sintering at different temperatures. The SEM images of the sintered fireclay samples show a decrease in pores or voids compared to raw fireclay due to the phenomenon of sintering. In case of Scanning Electron Microscope (SEM), image is formed by scanning the sample with a beam of electrons, which interact with the electrons of the sample to produce various signals which can be detected by a detector. The signals provide an idea regarding the surface morphology of the sample and its composition. For SEM, a powdered sample is taken on carbon tape which is mounted in a sample holder and the sample must be electrically conductive and grounded to prevent the accumulation of charge at the surface. For non-conductive samples, a coating of conductive material (palladium) is applied.

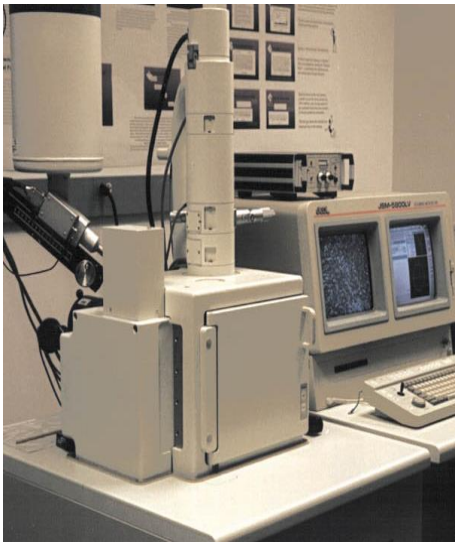

Fig 10. Scanning Electron Microscope

- **Raising Hearth Furnace:** The sintering of the fireclay specimens at various temperatures with varying soaking times has been performed using the raising hearth furnace. The maximum temperature of this furnace is 1650^0C. It consists of mounted platform with a furnace section having its opening at the bottom. The temperature change is controlled by a computer-controlled program. In order to charge the sample, the platform is lowered and then the furnace is closed by moving the hearth upwards into the heating cavity

Fig 11. Raising Hearth Furnace

CHAPTER-6
EXPERIMENTAL WORK

The present study deals with the investigation of different factors viz. particle size distribution, sintering temperature, and soaking duration on the properties of fireclay refractories. The raw materials used in all the experiments were fireclay grog and raw fireclay. The XRD analysis of the fireclay raw material has confirmed the presence of mainly sillimanite (Al_2SiO_5), quartz (SiO_2), and $NaTiO_2$ phases [15].

The grog was crushed using a jaw crusher and then the grog particles were sieved into desired size fractions by passing the grounded samples through a set of standard sieves placed in an automatic sieve shaker. The separation of the particles into three different size fractions is mentioned below. Moreover, the mass of the sample retained in each sieve during sieving was measured to determine the sieve distribution curve of the fireclay grog.

Table2. Different size fractions involved in the study

Particle Type	Particle size range	Sieve number (in BSS)
Coarse	-4mm to +0.5mm	-4+30
Medium	-0.5mm to +0.18mm	-30+80
Fine	-0.18mm	-80

Several batch compositions were determined by varying the percentage of coarse, medium, and fine-size fractions of the sample. In this study, bentonite clay was used as the binder to properly agglomerate the particles of the mixture. Initially, the dry mixing of the weighed amount of coarse and medium particles was done uniformly in an enamel tray. This is done to ensure that the medium particles fill the void spaces in between the coarse particles. Then after dry mixing bentonite clay was added as a binder along with 10-12% water (by weight) followed by the addition of the weighed amount of fine particles and then uniform mixing was performed to ensure the even distribution of the fine particles and sufficient wettability of the coarse grains by the binders. The semi-dry mixture was then filled in a cylindrical mold (having a specific dimension) and then pressed in a hydraulic press to obtain cylindrical briquettes having height and diameter **15mm** and **5mm** respectively [32].

The die, punch, and base were cleaned with acetone. The die was put on the base plate and weighed amount of powder was put in the die. The punch was inserted and slightly pressed down to touch the powder sample. The powder was pressed at 333 MPa load. The pressed article was carefully ejected and the dimensions of the green samples were measured with the help of Vernier calipers. After pressing the samples were dried at 110^0C.

After drying the samples were fired at different sintering temperatures (1250^0C, 1350^0C, 1450^0C) in a suitable furnace and then the diameter and height of the cylindrical pressed samples were determined to calculate the firing shrinkage. The bulk density and apparent porosity of the fired specimens were calculated by Archimedes principle with water as the immersion fluid.

Fig 12. Pressed green Sample ***Fig 13. Pressed fired sample***

Bulk Density and Apparent Porosity determination:

There are two methods regarding the determination of the above two properties:

- Boiling Method
- Vacuum Method

Both the methods are similar in terms of measuring conditions and parameters but the difference lies in their methodology part. In case of vacuum method, the immersed samples are placed in vacuum instead of boiling the samples. Boiling method is not applicable in case of other liquids (like kerosene and xylene) as immersion liquids due to their high rate of evaporation. Vacuum method becomes necessary for samples having greater hydration tendency where organic liquids are used as immersion liquid. In our experiment the bulk density and apparent porosity of the fired samples were determined by boiling water method using water as the immersion liquid. The methods involved in the determination of Bulk Density and Apparent Porosity are explained below:

- The fired specimen was dried at 110^0C till constant weight was obtained and the dry weight (D) of the specimen was noted down.
- The dried specimen was then suspended using copper wire in a beaker containing distilled water in a manner such that the specimen was completely covered with water and there was no contact between the surfaces of the specimen and the container.

- The beaker containing the water was heated and the water was allowed to boil for 2 hrs. The water level was maintained by adding water from outside to ensure that the specimen remains completely immersed in water. The boiling was done to remove the air from the surface pores of the specimen for accurate calculations of porosity.
- The beaker was then cooled down and the suspended weight (S) of the specimen was noted.
- The specimen was then removed from the water and gently wiped with tissue paper. Then the specimen was again weighed in a balance. This weight corresponds to the soaked weight (W) of the specimen [33].

Using the value of weights of the specimen under different conditions the Bulk Density and Apparent Porosity of the specimen were calculated using the formula stated below:

$$\textbf{Bulk Density}(\textbf{BD}) = \frac{\textbf{D}}{(\textbf{W} - \textbf{S})}$$

$$\textbf{Apparent Porosity}(\textbf{AP})\% = \frac{(\textbf{W} - \textbf{D}) \times \textbf{100}}{(\textbf{W} - \textbf{S})}$$

Here term (W-S) denotes the bulk volume of the sample and (W-D) denotes only the volume of the surface pores present in the specimen.

Determination of Volume Shrinkage:

Firing shrinkage refers to the dimensional change that occurs in the specimen after firing. Several parameters such as sintering temperature, composition, soaking duration, etc. affect the shrinkage value. This is an important property for the refractory manufacturer to adjust the mold dimensions to maintain the required dimension of the fired products. Shrinkage occurs during the heat treatment mainly due to the reduction in pore volumes from the sample. High shrinkage values can lead to the risk of cracks in the sample and thus should be avoided by proper compaction methods to minimize the shrinkage values [1].

$$\textbf{Volume Shrinkage} = \frac{(\textbf{Vg} - \textbf{Vf}) \times \textbf{100}}{\textbf{Vg}}$$

Here V_g = Volume of green sample

V_f= Volume of fired sample

Volume shrinkage is generally expressed in the form of a percentage.

Fuller Distribution:

In our study, the Fuller curve method is used to predict the appropriate ratio of coarse, medium, and fine fireclay particles in the feed which will provide the best compaction of the pressed and fired fireclay samples. Higher compaction will lead to fewer voids and thus lower apparent porosity values. In this method several feed mixtures with varying proportions of coarse, medium, and fine particles along with a certain amount of binder (which is bentonite in this case). The size distribution of each of the feed mixtures was determined using sieve analysis and through the sieve analysis data, the grading curves were drawn about the ideal Fuller curve [34]. In this way, the grading curves of the other feed mixtures were drawn. The curve which showed the least deviation from the ideal Fuller curve was selected and the corresponding mixture was selected as the optimized mix to form the most compact fireclay specimen. The deviation of the grading curves from the ideal curve was determined by two parameters namely, Coefficient of uniformity (CU) and Root mean square deviation (RMSD) which are expressed as:

$$\mathbf{RMSD} = \sqrt{\frac{\sum (\mathbf{X1} - \mathbf{X2})^{\mathbf{2}}}{\mathbf{n}}}$$

where X1 and X2 are the **% passing through** values of feed and ideal Fuller distribution respectively and n denotes the number of standard sieves involved in the analysis.

$$\mathbf{CU} = \mathbf{D60}/\mathbf{D10}$$

where D60 and D10 represent the screen size for which 60% and 10% of the sample are smaller respectively.

The grading curve with maximum CU value and minimum RMSD value will be considered the best mix for compaction. The curves that show deviation above the ideal Fuller curve indicate the presence of more fines whereas the curves that show deviation below the Fuller curve indicate the presence of fewer fines in the mixture [34]. The optimization of the mix was done based on CU and RMSD values and then the cylindrical specimen was prepared with the mixture by using a hydraulic press and then the apparent porosity of the specimen was determined by the above-mentioned method to validate the best compactness of the mixture

The experimental works involved in this study can be represented by a block diagram shown below:

Table 3. Flow diagram showing the different experimental works involved

:

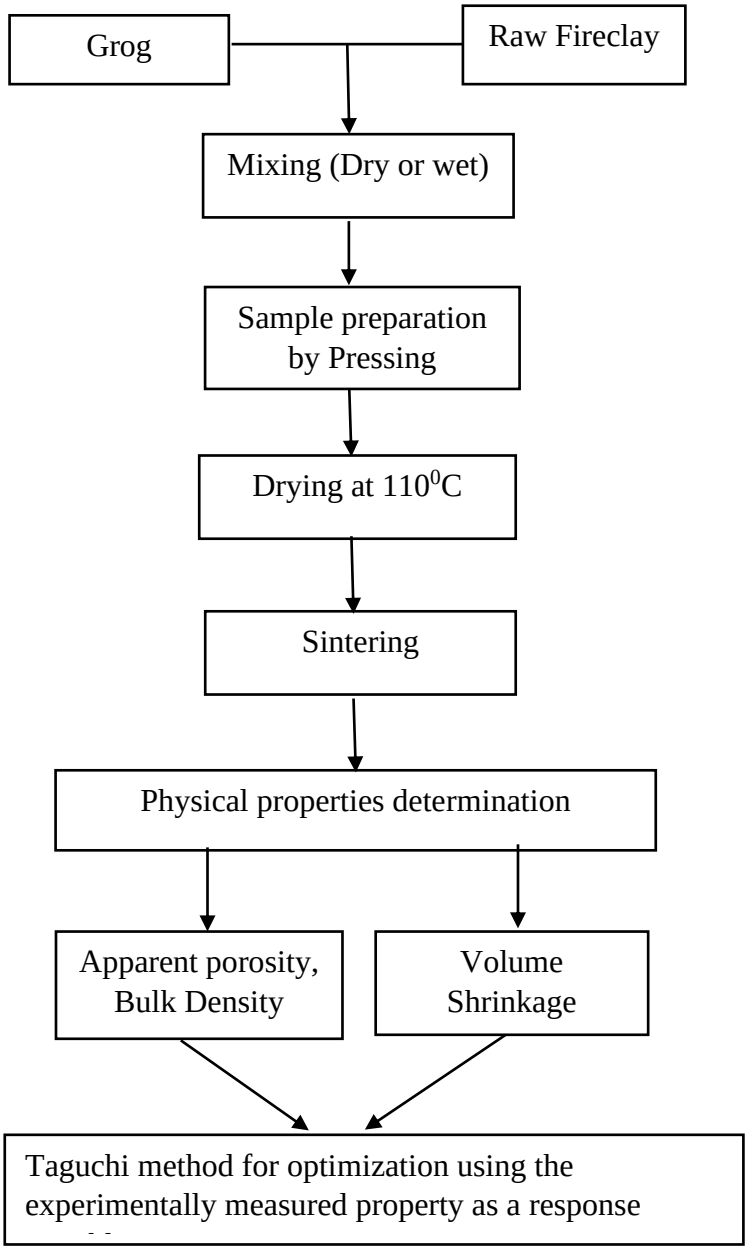

CHAPTER-7
RESULTS AND DISCUSSION

The present section describes the effect of the different variables viz, particle size distribution, sintering temperature, and soaking duration on the mechanical properties of fireclay bricks. Here the response parameter is apparent porosity which has been measured under different conditions to investigate their effects. Apart from these, the optimizations have been performed using Fuller distribution and Taguchi modeling to obtain the optimized set of conditions for the best results. Here the mechanical strength has not been directly measured instead apparent porosity has been chosen due to the ease of measurement. For our convenience, the pressing load has been kept constant in all the cases.

The experimental work included the formation of cylindrical briquettes of varying compositions at a constant pressing load. Then the samples were sintered at different temperatures leading to a shrinkage in the samples accompanied by a decrease in porosity (which will be discussed in the later section).

Several studies have revealed that a batch composition involving 40-45% coarse, 10-20% medium, and 40-45% fine fraction has achieved a maximum density close to the theoretical density. Thus, the fireclay samples were prepared considering the above-mentioned compositions (C: M: F) as a reference which are mentioned below:

- 50:10:40
- 60:20:20
- 40:20:40
- 50:30:20
- 40:20:30

The samples prepared using the above compositions were fired at different temperatures and then after sintering their volume shrinkage and apparent porosity were measured. A higher shrinkage value means a greater extent of sintering and lesser porosity which ultimately contributes to the strength of the refractory body. The temperature range for sintering has been chosen between 1250-1450^{0}C because temperatures exceeding 1500^{0}C can lead to the undesirable softening of the samples. A microstructural change occurs is expected to occur in the fireclay samples after sintering which will ultimately lead to an increase in strength. In this work two types of optimization techniques have been applied, one is the Fuller distribution method in order to achieve the best possible particle size distribution (on the basis of coarse, medium, fine sizes) in order to achieve the densest mixture for pressing and the other is Taguchi method which is utilized to determine the set of optimized parameters for best results (here minimum porosity) and the most influencing parameter. These things will be discussed in detail in the later part of this chapter.

Particle size distribution: In this study, the raw fireclay grog was crushed and then screened into different size fractions. For the determination of the average particle size, a weighed amount of raw fireclay was passed through a series of sieves, and the material retained in each sieve was weighed. The values obtained are represented in a tabular form below:

Table 4. Sieve analysis results of fireclay

Nominal aperture size (N) in mm	**Weight retained in sieve (gm)**	**% Weight retained in sieve (f_i)**	**Cumulative percentage finer**
4	0	0	100
3.675	49	13.88	88.11
2.675	53.7	15.21	74
1.85	19.4	5.49	65.41
1.55	44.6	12.63	57.78
1	25.6	7.25	47.52
0.55	14.5	4.10	40.42
0.4	34.9	9.88	31.53
0.275	28.4	8.04	23.5
0.231	10	2.83	20.65
0.196	8.5	2.40	18.24
0.153	15.6	4.41	13.82
0.115	10	2.83	11
0.089	5.8	1.64	9.35
0.069	12.8	3.62	5.723
0.051	11.9	3.37	2.36
0.0317	5.4	1.53	0.822
0.02	2.4	0.68	0

The nominal aperture was calculated by considering the average value of the two sieve openings. The particle size distribution curve can be expressed both in terms of cumulative % undersize and cumulative % oversize but in this study the former has been used.

The average particle size has been determined using the following equation:

$$\textbf{Average particle size} = \frac{\sum_{i=1}^{n} \mathbf{fi}}{\sum_{i=1}^{n} \mathbf{fi}/\mathbf{Ni}}$$

By inserting the values of f_i and N_i in the above equation the calculated average particle size was found to be 0.28 mm.

:

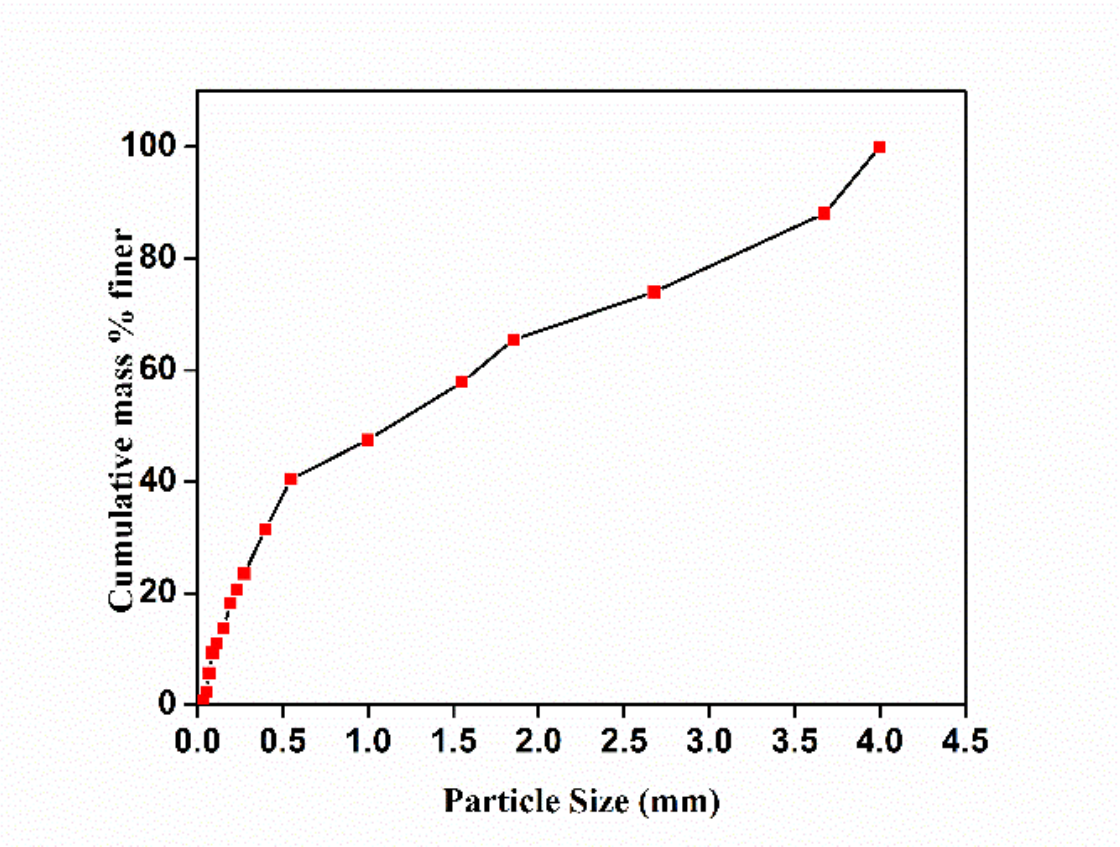

Fig 14: Particle size distribution curve of raw fireclay

Volume Shrinkage: The volume shrinkage has been calculated simply by determining the difference in the volumes of the fireclay samples before and after sintering. In sintering the particles come in close contact with each other which leads to the reduction in volume of the specimens. The pressed samples for this study were cylindrical as a result of which their volumes were determined by the equation:

$$\textbf{Volume}(\mathbf{V}) = \frac{\pi \mathbf{d}^2 \mathbf{h}}{4}$$

(Where d and h denote the diameter and height of the samples respectively)

Three sets of fireclay samples were prepared for each of the different compositions mentioned above, and they were sintered at temperatures 1250^0C, 1350^0C, and 1450^0C. The dimensions of the samples before and after sintering were noted down and their volume shrinkage was determined. The results are represented in a tabular form below:

Table 5: Volume Shrinkage results at different temperatures

Temperature	50:10:40	60:20:20	40:20:40	50:30:20	45:10:45
1250^0C	2.23	5.37	3.92	1.80	8.89
1350^0C	3.87	8.324	7.43	2.65	14.73
1450^0C	3.96	8.762	8.07	2.90	15.24

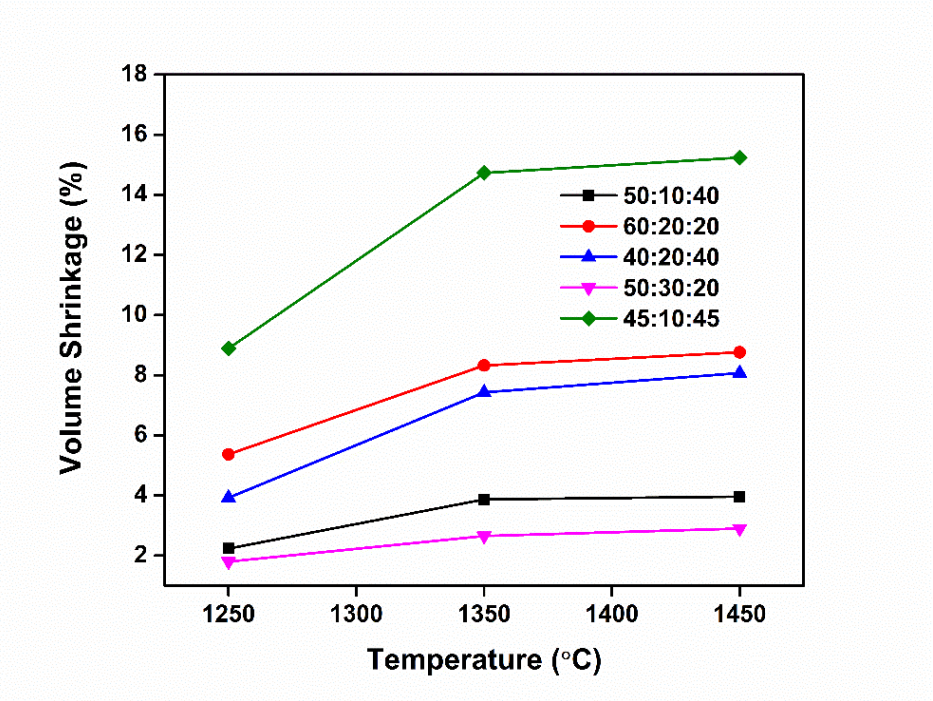

Fig 15: Variation of volume shrinkage with temperature for different composition

The plot of the volume shrinkage vs temperature for different compositions suggested that in general for any composition the shrinkage was lowest at 1250^0C. However, as the sintering temperature was increased from 1250^0C to 1350^0C a sharp increase in the shrinkage value was observed mainly due to the initiation of sintering. The increase in shrinkage can also be attributed to the formation of a liquid glassy phase which leads to the reduction and blockage of the pores. (Tabit et al., 2018) [35]. As the temperature was further increased to 1450^0C a slight increase in the volume shrinkage of the samples was observed. From the graph it is evident that the highest shrinkage values are observed for the sample having composition 45:10:45. Highest shrinkage was observed for the composition 45:10:45 sintered at

1450^0Cwhich indicated the greatest extent of sintering due to the presence of a relatively large percentage of fines.

The increase in volume shrinkage with temperature can be explained by the closeness of the particles due to sintering accompanied by the emergence of the liquid phase. On cooling, the liquid glass freezes which also results in a decrease in apparent porosity values (which will be discussed later) [20].

To observe the variation of volume shrinkage with soaking duration, samples of different compositions were sintered at definite temperatures with various soaking times viz, (30mins, 45mins, and 60mins) and then their volume shrinkage was measured by the same procedure. In this case total of three sets (each comprising two different compositions) of experiments were sintered at a particular temperature in different soaking intervals in the following arrangement:

Set 1 (Sintering temperature 1250^0C):

a) 45:10:45
b) 50:20:30

Set 2 (Sintering temperature 1350^0C):

a) 40:20:40
b) 50:30:20

Set 3 (Sintering temperature 1450^0C)

a) 50:10:40
b) 60:20:20

The volume shrinkage values obtained are represented in a tabular form below:

Table 6: Volume Shrinkage results at different soaking time

Soaking time (minutes)	**45:10:45 (1250^0C)**	**50:20:30 (1250^0C)**	**40:20:40 (1350^0C)**	**50:30:20 (1350^0C)**	**50:10:40 (1450^0C)**	**60:20:20 (1450^0C)**
30	7.43	6.26	10.26	8.33	8.83	9.51
45	8.6	7.84	12.54	9.59	10.34	11.37
60	7.76	7.36	11.42	8.65	9.96	10.86

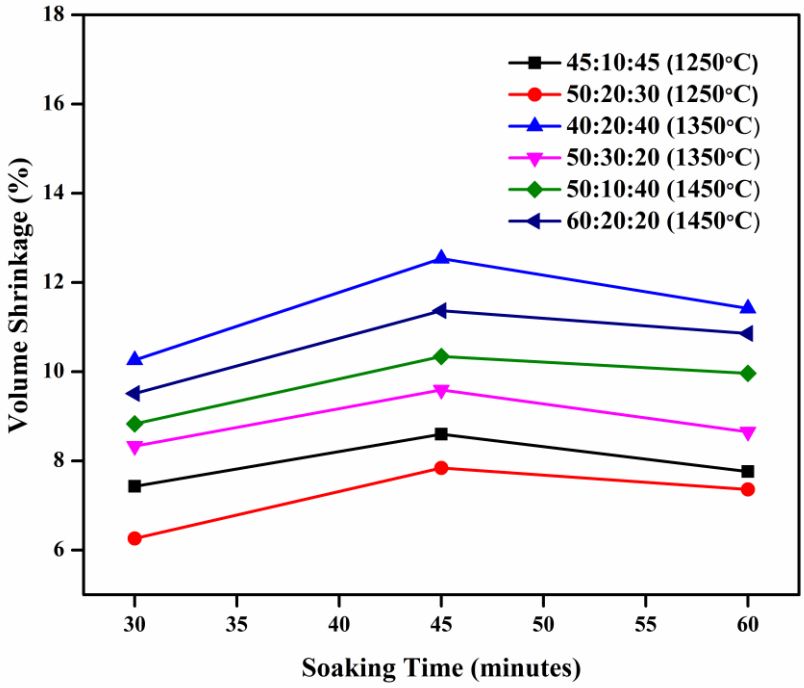

Fig 16: Variation of volume shrinkage with soaking time for different compositions

The plot of the volume shrinkage vs soaking duration suggested that volume shrinkage was highest at a soaking duration of 45 minutes irrespective of batch composition and sintering temperature. The samples sintered at high temperatures showed high volume shrinkage values. In this case, the highest set of shrinkage values was observed for sample 2a (mentioned earlier).

Apparent Porosity: The apparent porosity was determined using the Boiling Water method according to Archimedes' principle. The apparent porosity was calculated using the following equation:

$$\textbf{Apparent Porosity}(\textbf{AP})\% = \frac{(\textbf{W}-\textbf{D})\times \textbf{100}}{(\textbf{W}-\textbf{S})}$$

(Where 'D', 'W' and 'S' denote the dry weight, soaked weight and suspended weight respectively).

Here three samples were prepared for each of the different compositions and they were sintered at temperatures 1250^0C, 1350^0C and 1450^0C**.** The obtained apparent porosity values are represented in a tabular form below:

Table 7: Apparent Porosity results at different temperatures

Temperature	50:10:40	60:20:20	40:20:40	50:30:20	45:10:45
1250^0C	12.34	9.56	8.45	10.35	7.9
1350^0C	8.57	6.84	5.46	7.38	4.35
1450^0C	6.86	5.6	4.57	6.56	2.83

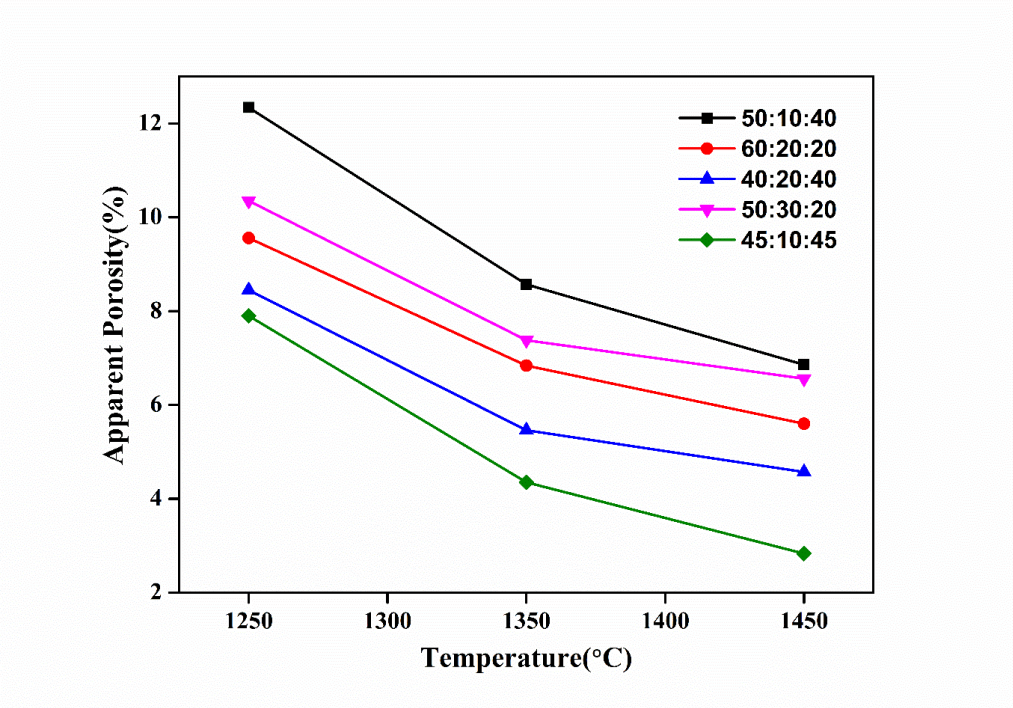

Fig 17: Variation of apparent porosity with temperature for different compositions

The graph clearly indicates a decreasing trend in apparent porosity with increase in sintering temperature irrespective of any batch composition. Highest porosity was observed for the fireclay samples sintered at low temperature (in this case 1250^0C) however increase in sintering temperature resulted in a decrease in apparent porosity due to densification and elimination of pores. Lowest set of apparent porosity values were observed for the samples with batch composition 45:10:45 which indicates significant compaction. The lowest apparent porosity value observed was 2.83% at 1450^0C.

In order to observe the variation of apparent porosity with soaking duration, samples of different compositions were sintered at definite temperatures at various soaking times viz, (30mins, 45mins and 60mins) and then their apparent porosity was measured

Table 8: Apparent Porosity results at different soaking times

Soaking time (minutes)	45:10:45 (1250^{0}C)	50:20:30 (1250^{0}C)	40:20:40 (1350^{0}C)	50:30:20 (1350^{0}C)	50:10:40 (1450^{0}C)	60:20:20 (1450^{0}C)
30	8.30	9.97	3.468	4.35	8.5	6.9
45	5.74	7.86	2.31	4.70	5.75	4.96
60	9.10	10.03	4.46	2.24	6.367	4.59

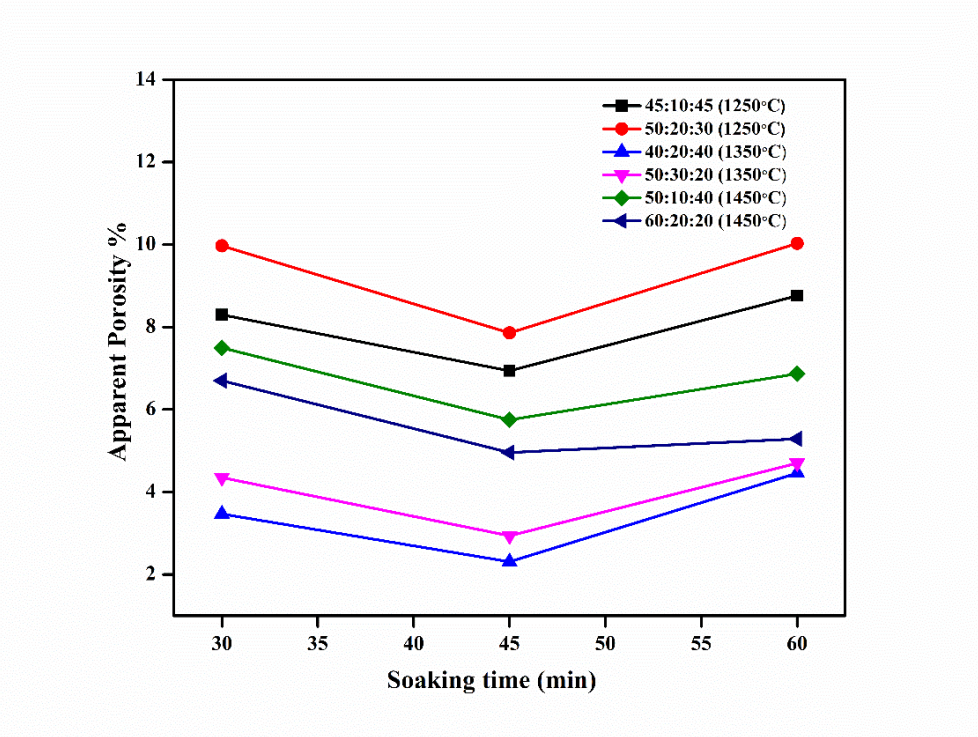

Fig 18: Variation of apparent porosity with soaking time for different compositions

The graph shows that the lowest apparent porosity values are obtained for the samples sintered at a soaking duration of 45 minutes. The apparent porosity value initially showed a sharp decrease as the soaking duration increased from 30 min to 45 mins beyond which a slight increase in the porosity value was observed. The lowest apparent porosity was observed for the sample 2b sintered for 45 minutes.

Characterization Techniques: Different characterization techniques viz, Scanning Electron Microscopy (SEM) and X-ray diffraction (XRD) were adopted to analyze the raw fireclay and sintered fireclay specimens.

XRD characterization: The XRD images of raw fireclay have confirmed the presence of Silica, Quartz, and Sillimanite as the major phases [36]. The XRD patterns of the sintered fireclay however have shown the mullite as the major phase along with some amount of silica. The appearance of the peaks corresponding to the mullite phase in the XRD images of the sintered samples has indicated the phase transformation due to sintering. The mullite is the phase that is responsible for the high mechanical strength of the sintered specimens.

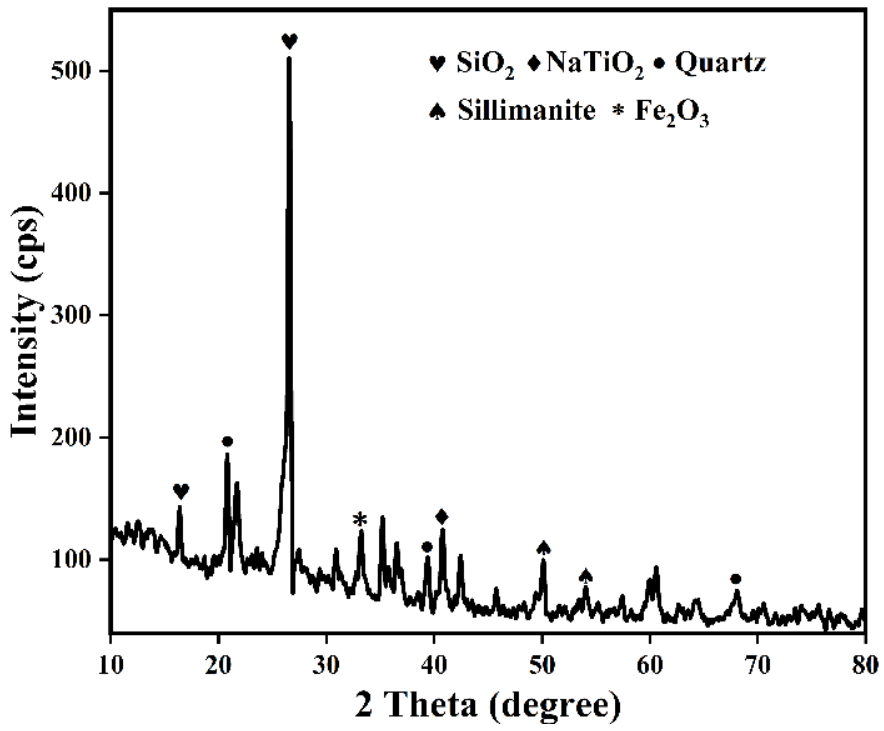

Fig 19: XRD patterns of raw fireclay

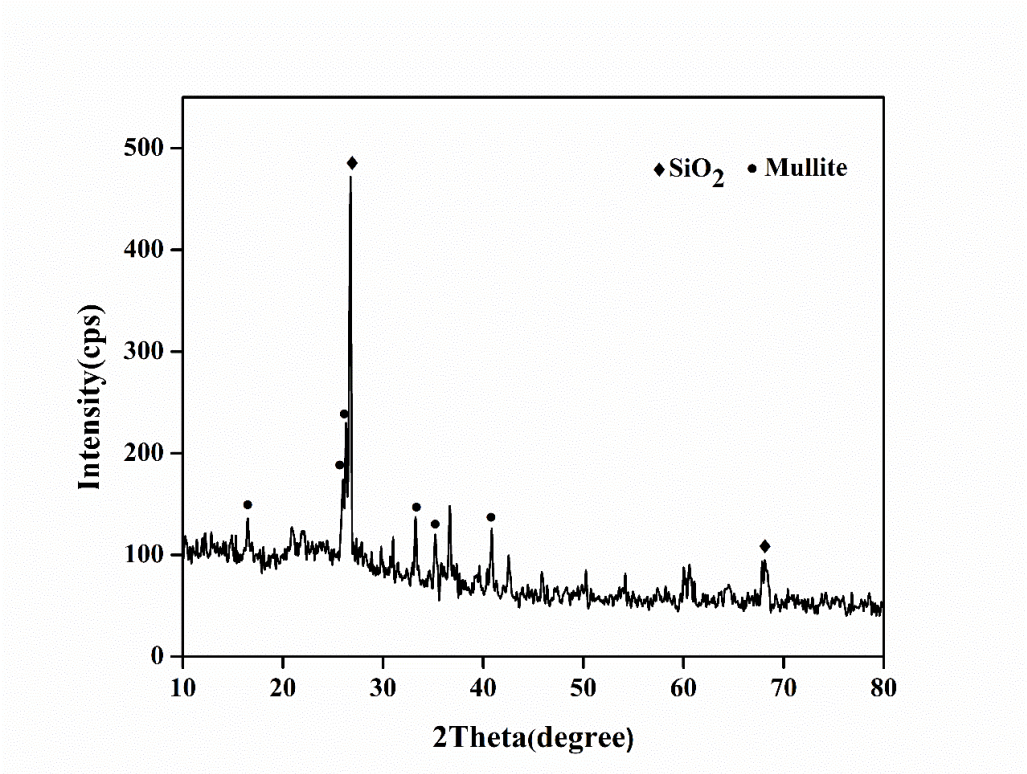

Fig 20: XRD patterns of sintered fireclay 1350^{0}C

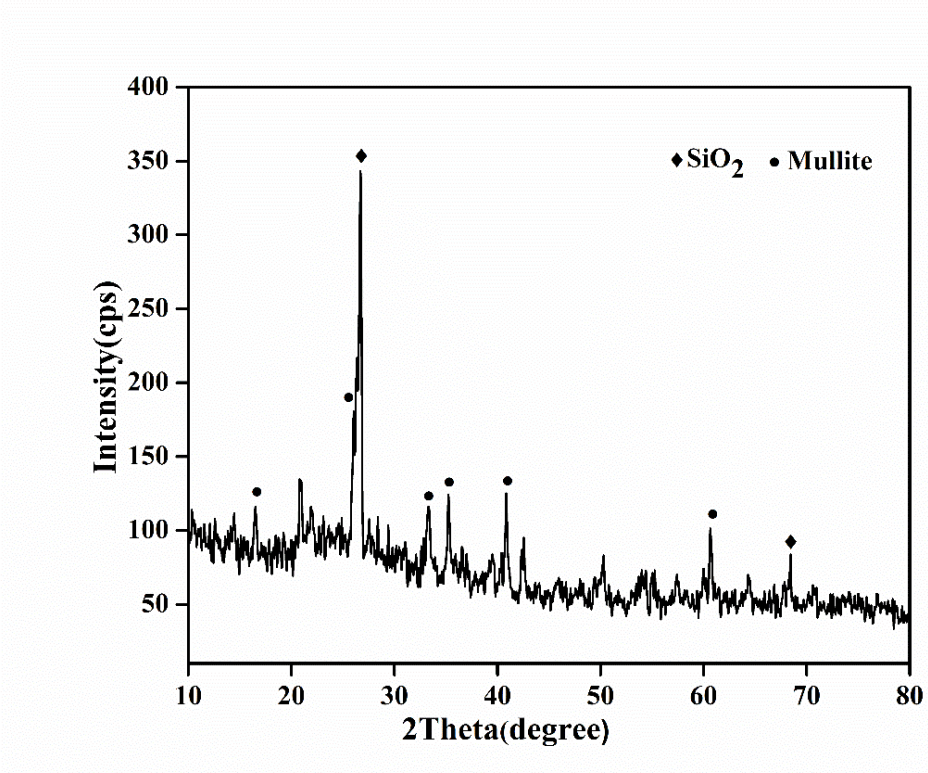

Fig 21: XRD patterns of sintered fireclay 1450^{0}C

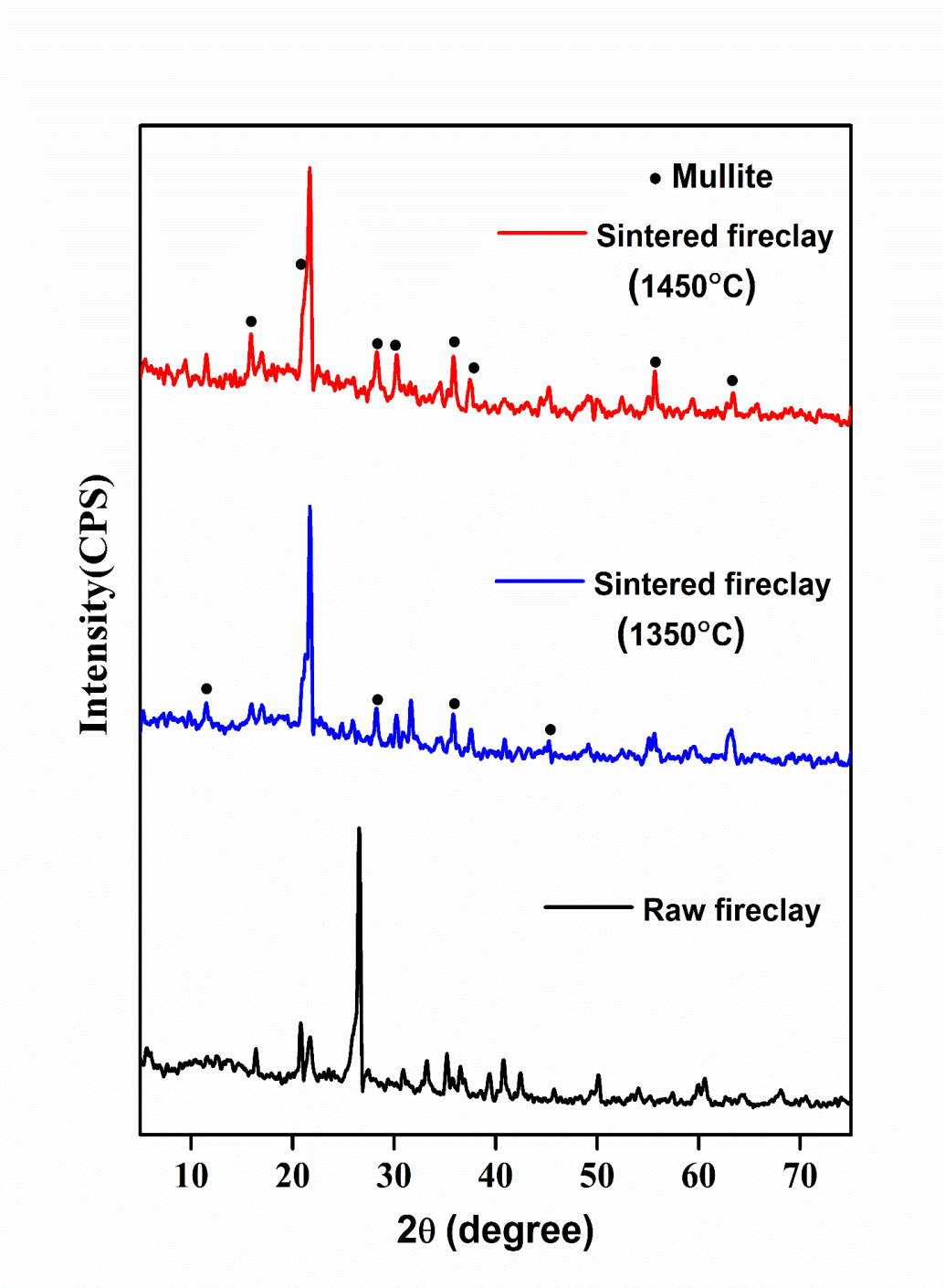

Fig 22: Comparative XRD patterns of fireclay under different conditions

XRD analysis of the fireclay specimens at different temperatures:

The comparative XRD analysis of fireclay specimens at different temperatures revealed the presence of the mullite phase at only high temperatures. The figure revealed no presence of mullite phases for raw fireclay however, mullite peaks were observed in case of fireclay samples fired at temperatures 1350^0C and 1450^0C which indicated significant phase transformation due to sintering. The frequency of the mullite peaks increased with an increase in temperature indicating the greater extent of sintering with the increase in temperature [37].

SEM characterization: The SEM analysis was used to study the surface morphology of the particles. The SEM images revealed the existence of voids in case of raw fireclay. However, a considerable decrease in voids was observed due to sintering. With increase in sintering temperature an improvement on surface morphology and densification can also be concluded from the SEM images. The sintering of refractory materials improves the strength, due to the reduction of pores and closer packing between the particles [38].

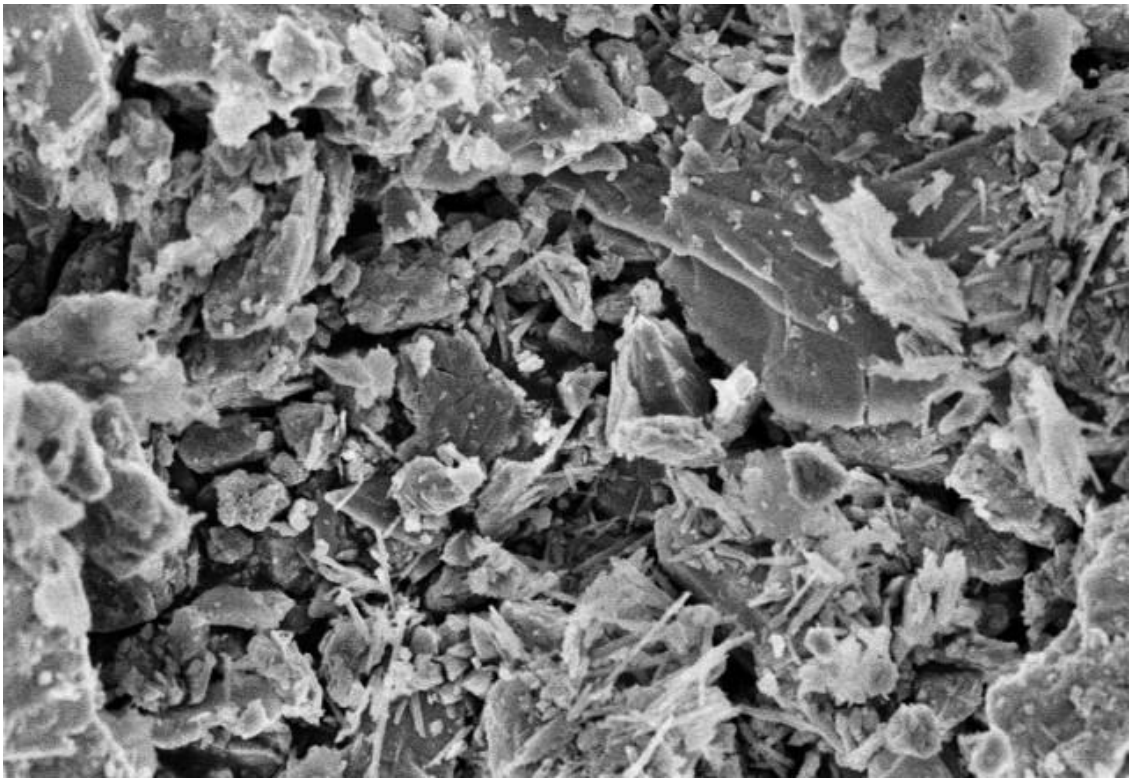

Fig 23: SEM image of raw fireclay

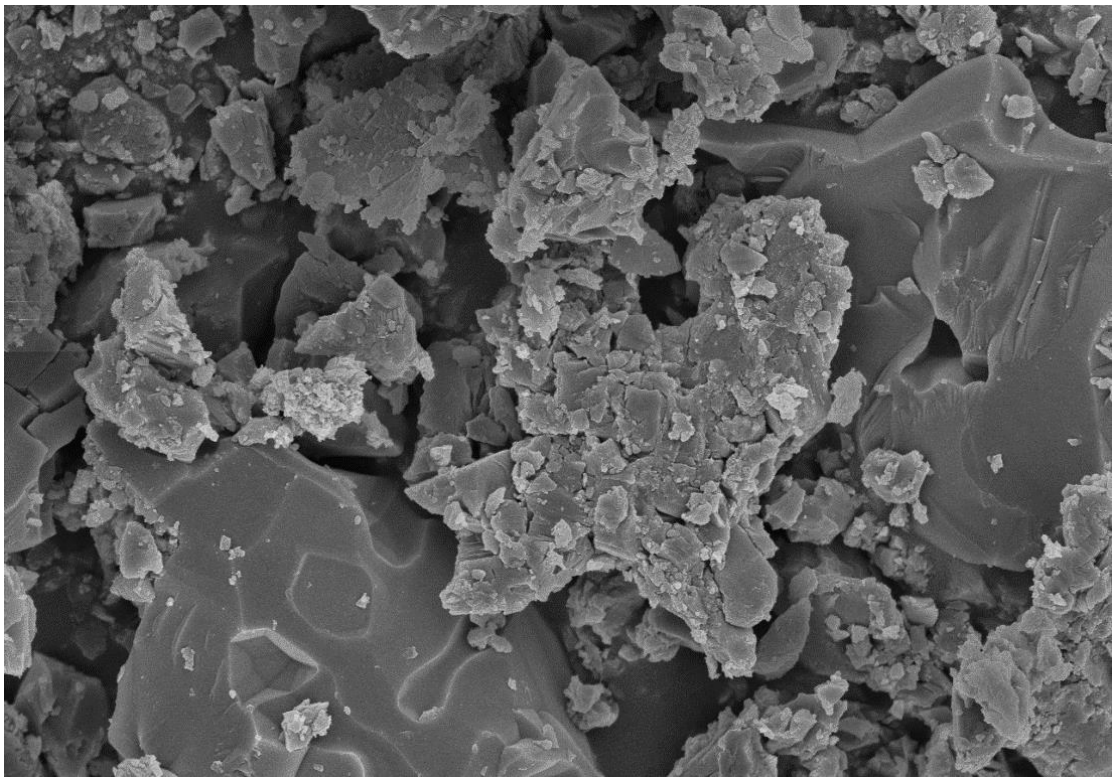

Fig 24: SEM image of sintered fireclay at 1350^{0}C

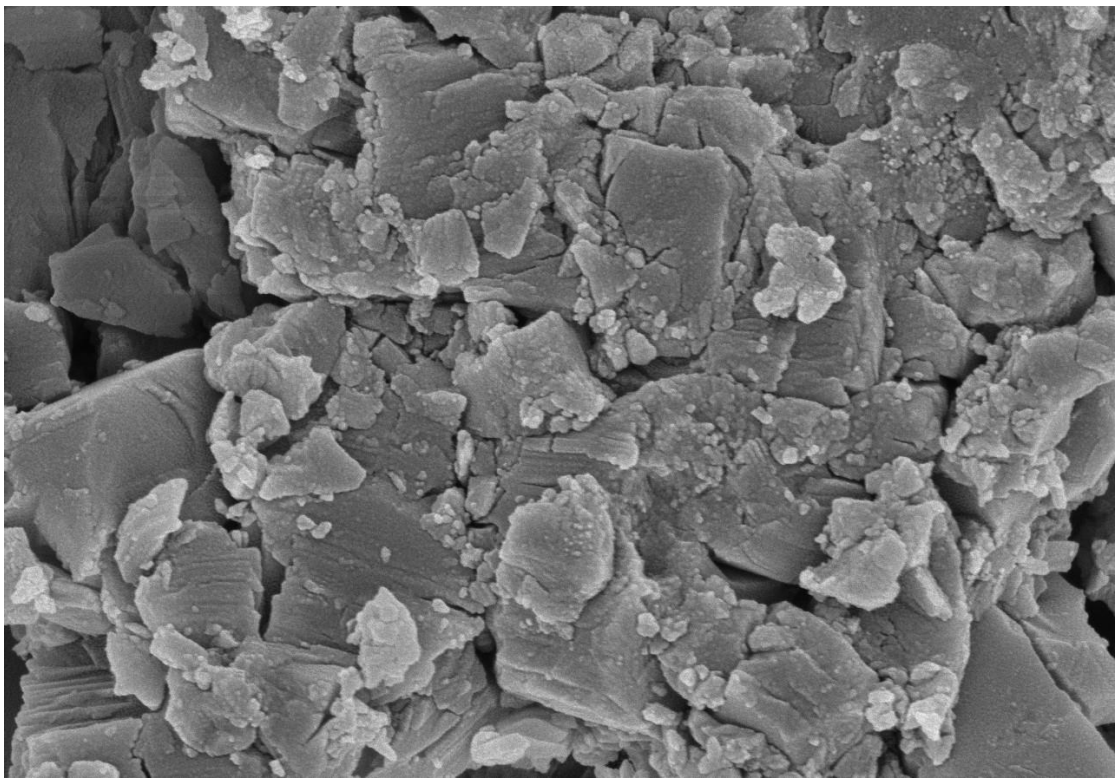

Fig 25: SEM image of sintered fireclay at 1450^{0}C

Fuller distribution: This method involves the comparison of the size distribution of a batch with the ideal Fuller curve. The size distribution of the different particles (coarse, medium, and fine) in the batch composition significantly affects the porosity (and hence mechanical strength) of the pressed samples and thus proper grading of the raw material is essential for achieving the highest packing density of the pressed fireclay samples. The ideal Fuller curve is obtained by plotting the ideal percentage of material through a set of standard sieves which is given by the equation:

$\mathbf{P = [Dx/Dmax]^{n} * 100}$ where P = % passing square aperture D_x

D_{max} = maximum particle size, mm n = grading co-efficient which is 0.5 in this case

Two parameters namely Root Mean Square Deviation (RMSD) and Co-efficient of Uniformity (CU) are mainly used to determine the best possible batch composition for sample preparation and they are given by the equations:

$$\mathbf{RMSD} = \sqrt{\frac{\sum (\mathbf{X1-X2})^{2}}{\mathbf{n}}} \qquad \mathbf{CU = D60/D10}$$

In the present study, several batches with varying percentages of coarse, medium, and fines were prepared, and their size distribution curves were determined using sieve analysis. The RMSD and CU values of each of the distribution curves were calculated and the curve that showed the least deviation from the ideal Fuller curve was chosen as the best fit [39]. Also, an attempt has been made for the correlation of RMSD and CU from the obtained data. The six different batch compositions taken are as follows:

A. 45:10:45
B. 60:20:20
C. 50:20:30
D. 40:20:40
E. 50:10:40
F. 50:30:20

The six compositions were mixed with a fixed amount of binder and the sieve analysis, RMSD, and CU results obtained are represented in a tabular form below:

Table 9. Particle size distribution of different batch compositions

Particle size (mm)	Fuller Distribution	Feed distribution (A)	Feed distribution (B)	Feed distribution (C)	Feed distribution (D)	Feed distribution (E)	Feed distribution (F)
4	100	100	100	100	100	100	100
3.675	95.851	88.11	95.35	94.7	90.35	99.35	96.35
2.675	81.77	74	89.51	78.51	83.61	93.51	86.17
1.85	68	65.41	81.97	69	60.97	85.97	78.97
1.55	62.25	57.78	78.54	65.54	53.5	81.54	74.54
1	50	47.52	67.96	53	39.97	67.96	61.96
0.55	37.08	40.42	46.68	33	29.67	46.68	32.38
0.4	31.62	31.53	23.3	26.2	19.27	35.3	26.8
0.275	26.22	23.5	17.54	15.52	15.45	21.54	21.54
0.231	24.03	20.651	17.95	14.75	18.32	17.95	18.07
0.196	22.136	18.244	14.44	14.68	14.36	24.44	18.57
0.153	19.557	13.82	15.35	12.85	15.37	15.35	15.48
0.115	16.955	11	9.59	10.37	9.63	9.59	9.79
0.089	14.91	9.35	7.21	7.25	5.22	7.21	8.21
0.069	13.133	5.723	5.723	6.26	5.73	9.723	8.743
0.051	11.29	2.36	2.33	2.38	2.38	2.36	4.37
0.0317	8.90	0.822	0.835	0.874	1.823	0.832	1.232
0.02	7.07	0.15	2.2	4.23	0.85	2.2	2.57
0	0	0	0	0	0	0	0
RMSD		5.35	8.57	6.13	7.5	9.31	6.74
CU		11.65	6.723	10.63	8.85	7.218	9.05

The distribution curves of the six different batch compositions are shown in the next pages. The deviation of each of the curve with that of the ideal Fuller curve was measured to ultimately determine the best suitable mix for compaction.

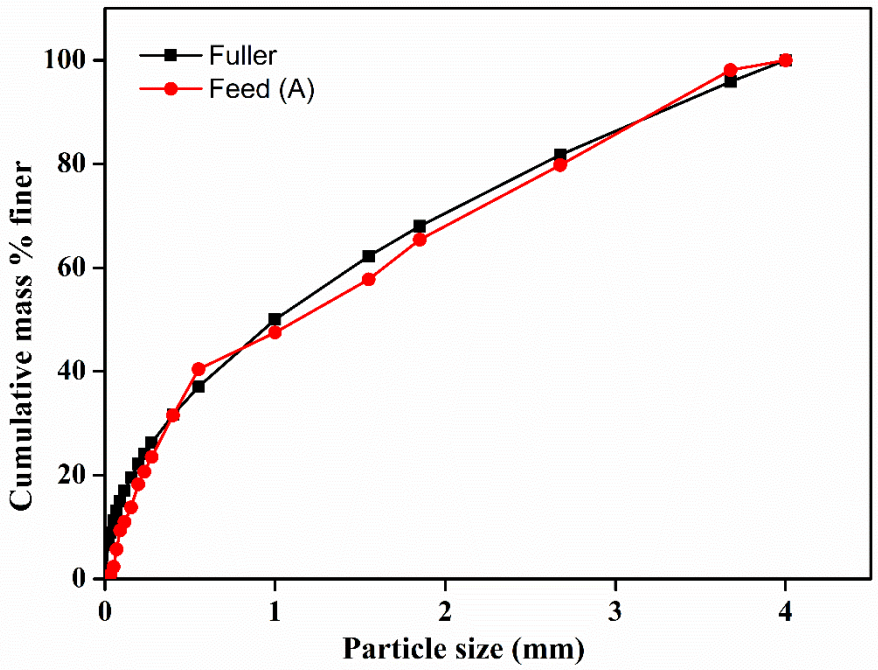

Fig 26: Fuller distribution curve of batch A

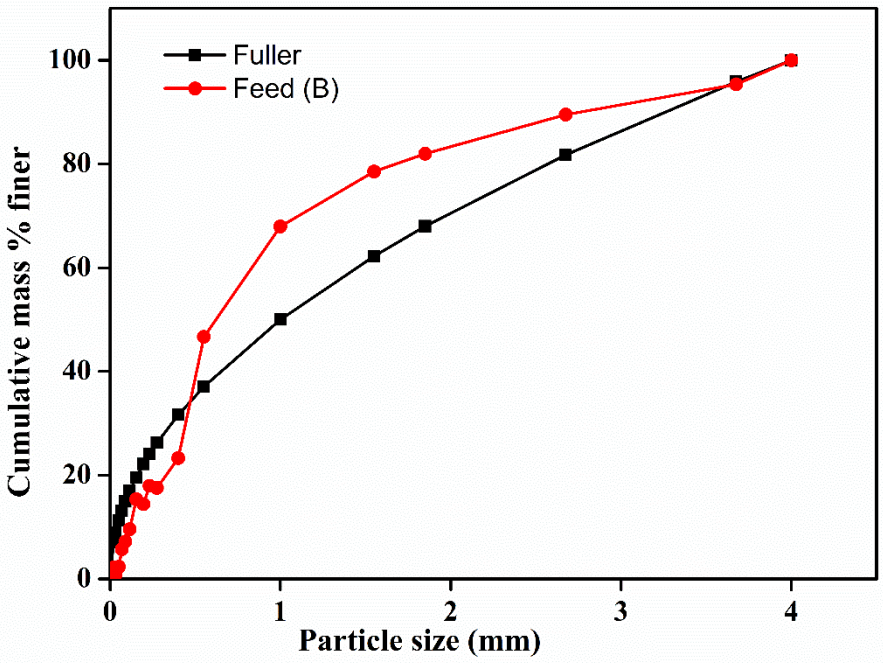

Fig 27: Fuller distribution curve of batch B

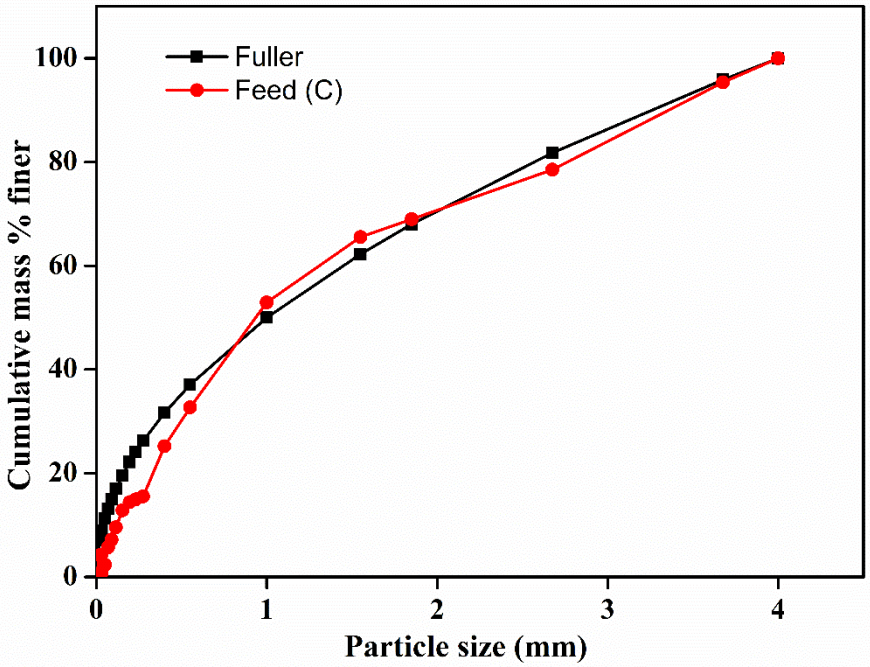

Fig 28: Fuller distribution curve of batch C

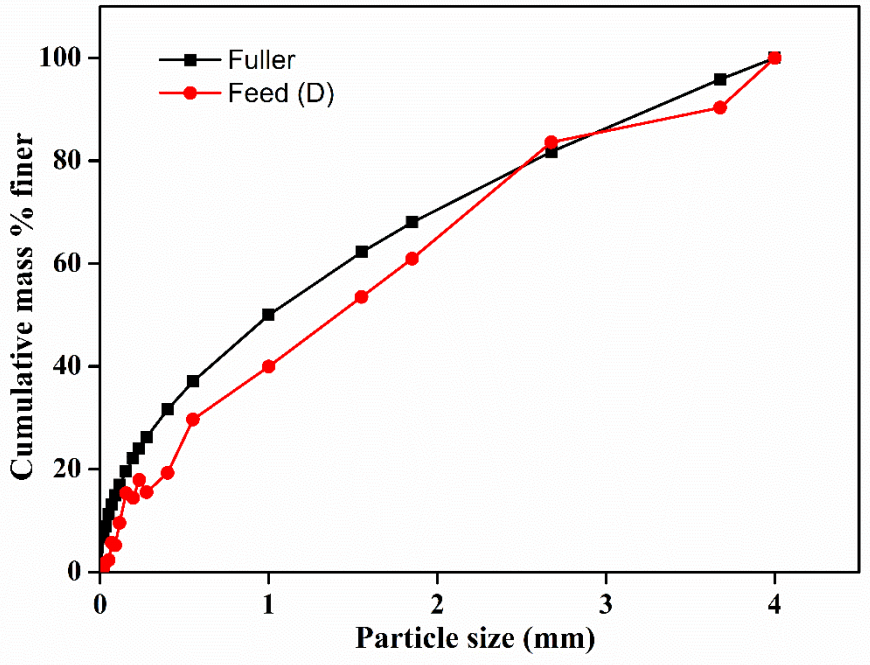

Fig 29: Fuller distribution curve of batch D

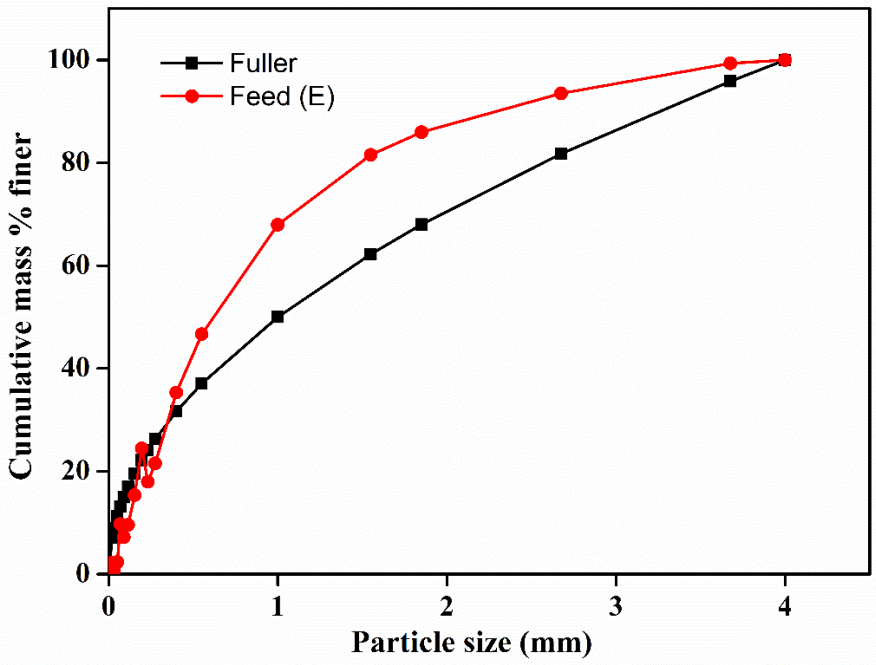

Fig 30: Fuller distribution curve of batch E

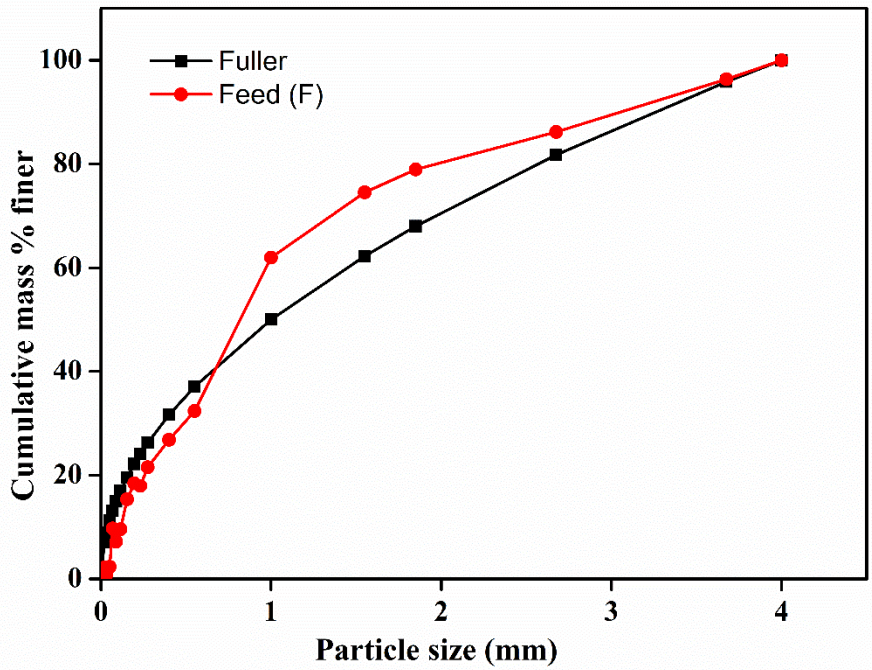

Fig 31: Fuller distribution curve of batch F

Fuller curve method is widely used in concrete technology for improvement of mechanical properties through proper particle size distribution. The same concept has been used in this study to produce the most compact fireclay briquettes.

For an ideal Fuller curve, the value of **Coefficient of Uniformity (CU)** is supposed to be **36** which is much higher compared to our experimental results. This deviation can be attributed due to the low particle size range (0.02 to 4mm) involved in our study. The grading curves positioned above the Fuller curve indicated the presence of more fines in the mix than the space between the coarse particles whereas the curves below the Fuller curve suggested the presence of fewer fines [39].

From the different curves obtained, the curve for the sample A showed the least deviation from ideality. The CU value and RMSD values obtained for the batch composition A were **11.65** and **5.35** respectively. The optimization was carried out based on CU and RMSD values. The mix with the lowest RMSD and highest CU value (which is mixture A in this case) was expected to give the best mechanical properties due to the minimization of the voids. The batch composition B showed the highest deviation with CU and RMSD values **7.218** and **9.31** respectively.

To **validate** our observation, pressed fireclay samples were prepared using the above six different batch compositions, and their apparent porosity values were calculated. In this case, the mechanical strength was not measured directly instead, the apparent porosity was considered as a measure of the mechanical strength. The apparent porosity value of the pressed sample with batch composition A was found to be the **lowest** which coincided with our expectations .

An attempt has also been made to correlate the two parameters Co-efficient of Uniformity (CU) and Root Mean Square Deviation (RMSD) involved in the Fuller distribution method. The different sets of CU and RMSD values obtained are represented in a tabular format below:

Table 10. Different sets of CU and RMSD values

CU	11.65	6,723	10.63	8.85	7.218	9.05
RMSD	5.35	8.57	6.13	7.5	9.31	6.74

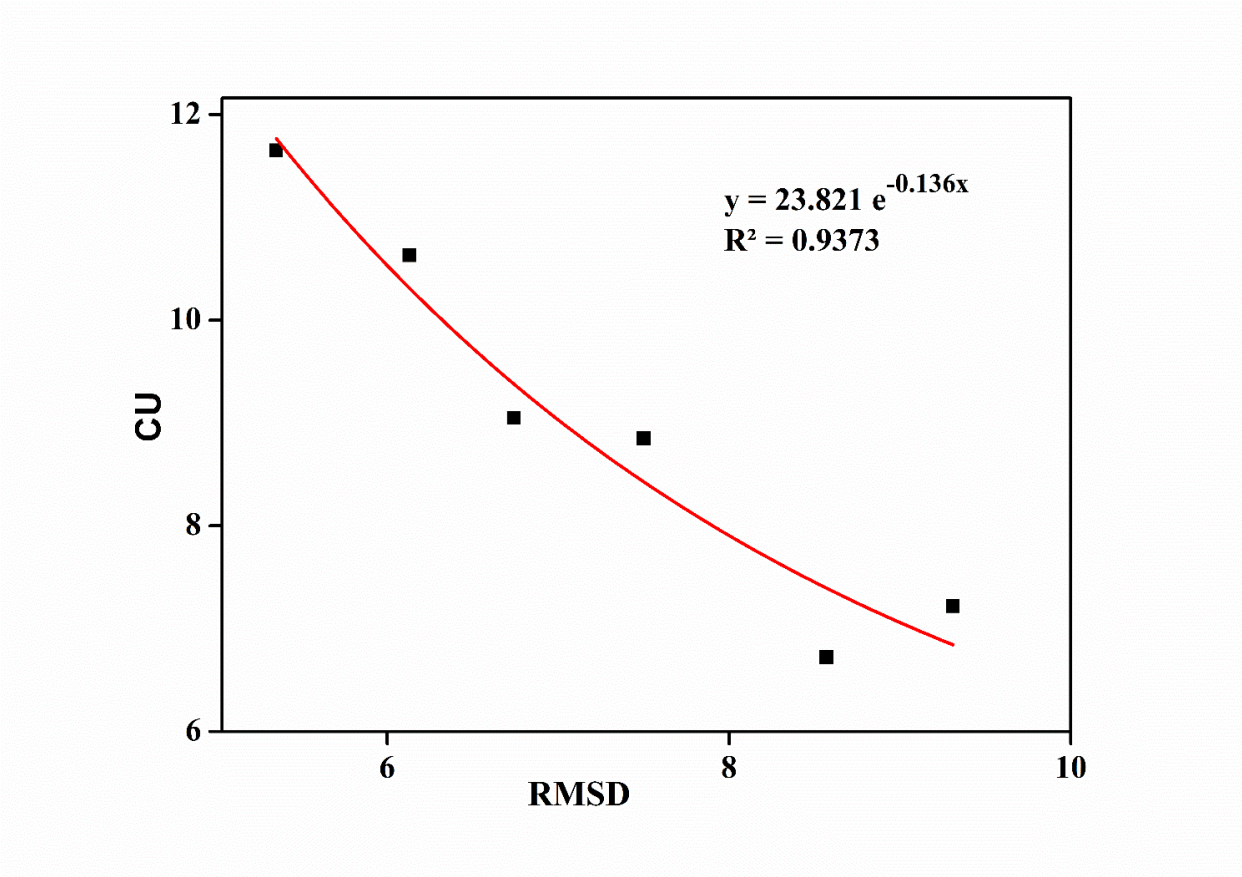

Fig 32: Correlation between CU and RMSD

The graph between CU and RMSD indicated an exponential relationship with an inverse variation. The exponential nature of the curve fitted well with the R^2 value 0.937. Thus, from the above study, the following points can be concluded:

- Higher CU value indicates less deviation from the ideal Fuller grading curve. The highest CU value of 11.65 was obtained in our study for batch composition A.
- RMSD is inversely proportional to CU. The lowest RMSD value of 5.35 was observed for batch composition A.

Thus, according to Fuller distribution, batch A with composition **45:10:45** was selected as the optimized batch.

Taguchi method: Taguchi is a very efficient experimental design which is used for single objective optimization problem. It is a multi-step process which involves the three stages namely, system design, parameter design and tolerance design. The Signal to Noise ratio provides a measure of the impact of noise factors on the performance. Three types of S/N ratio are mainly used: (a) Larger the Better (b) Smaller the Better (c) Nominal the Better. Depending upon the objective and response a particular type of S/N ratio is chosen for further analysis.

In our experimental study since the response variable, apparent porosity is desired to be minimum hence 'smaller the better' type of S/N ratio is used for optimization. The smaller the better type S/N ratio is expressed by the equation:

$$\frac{S}{N}ratio = -10\log_{10}(\frac{1}{n}\sum_{i=1}^{n} yi^2)$$

Where n denotes the number of replications and y is the observed data. The entire Taguchi method of optimization was conducted using a 'MINITAB' software.

The current study involved the investigation of the effect of different parameters on the mechanical properties of refractory materials. Here the experiment was carried out on fireclay refractory primarily due to ease of availability and lower fusion temperature. Apparent porosity was chosen as the output variable in this study for its indirect dependence on the mechanical strength. A total of 5 independent variables (each comprising of 3 levels) were taken into consideration with apparent porosity (AP) as the response variable. Thus a 5 factor 3 level design involving L-27 Orthogonal Array was applied and the response of the 27 different set of experiments were measured using standard procedures (discussed earlier) for minimization of AP [11]. Apart from this several other techniques like Response Surface Method (RSM), Analysis of Variance (ANOVA) were also applied to correlate the response variable with the different input parameters and determine the most significant factor(s). Lastly the confirmatory test was conducted to validate the optimization method [40]. The different input parameters used in this experiment are represented in a tabular manner as follows:

Table 11. Input parameters along with different level values

Input Parameters	Unit	Levels		
		Level 1	Level 2	Level 3
Coarse	%	(35-45) %	(45-55) %	(55-65) %
Medium	%	(0-10) %	(10-20) %	(20-30) %
Fine	%	(35-45) %	(45-55) %	(55-65) %
Sintering temperature	^{0}C	1250^{0}C	1350^{0}C	1450^{0}C
Soaking Duration	min	30	45	60

In order to study the effect of the input parameters on the apparent porosity (response variable) mean effect plots were drawn using the data in Table 13. The main effect plots for the **S/N** ratios suggest that minimum apparent porosity value (AP) with decrease in coarse percentage and increase in soaking duration.

On the contrary, with increase in sintering temperature the apparent porosity initially decreases and then increases. The same trend is observed for medium size fraction particles. The above observations can be explained due to the combined effect of all the input parameters which collectively influence the apparent porosity of the refractory body. The experimental response values for different experimental sets are represented in a tabular format as follows:

Table 12: Response values for different experiment sets

S/No	Input Parameters					Response
	Coarse (%)	Medium (%)	Fine (%)	Temp (^{0}C)	Time (min)	Apparent Porosity (AP)%
1	1	1	1	1	1	9.97
2	1	1	1	1	2	7.86
3	1	1	1	1	3	10.03
4	1	2	2	2	1	3.46
5	1	2	2	2	2	2.31
6	1	2	2	2	3	4.46
7	1	3	3	3	1	5.75
8	1	3	3	3	2	8.29
9	1	3	3	3	3	4.347

10	2	1	2	3	1	8.49
11	2	1	2	3	2	5.75
12	2	1	2	3	3	6.36
13	2	2	3	1	1	8.308
14	2	2	3	1	2	5.74
15	2	2	3	1	3	9.10
16	2	3	1	2	1	4.35
17	2	3	1	2	2	4.70
18	2	3	1	2	3	2.23
19	3	1	3	2	1	4.608
20	3	1	3	2	2	4.69
21	3	1	3	2	3	4.003
22	3	2	1	3	1	6.896
23	3	2	1	3	2	4.96
24	3	2	1	3	3	4.59
25	3	3	2	1	1	12.75
26	3	3	2	1	2	9.41
27	3	3	2	1	3	8.95

The smaller-the better criteria was selected for Apparent Porosity (AP) minimization. The main effect plot for the S/N ratio suggested the set of optimum parameters as follows: **$(Coarse)_1$, $(Medium)_2$, $(Fine)_1$, $(Sintering\ Temperature)_2$, $(Soaking\ time)_3$**. A higher mean of S/N ratio indicated a minimum variation difference between the desired output and measured output. Thus, from the higher mean values from the S/N ratio curve **in Fig 34** the optimal values were determined [40].

Fig 33: Main effects plot for means

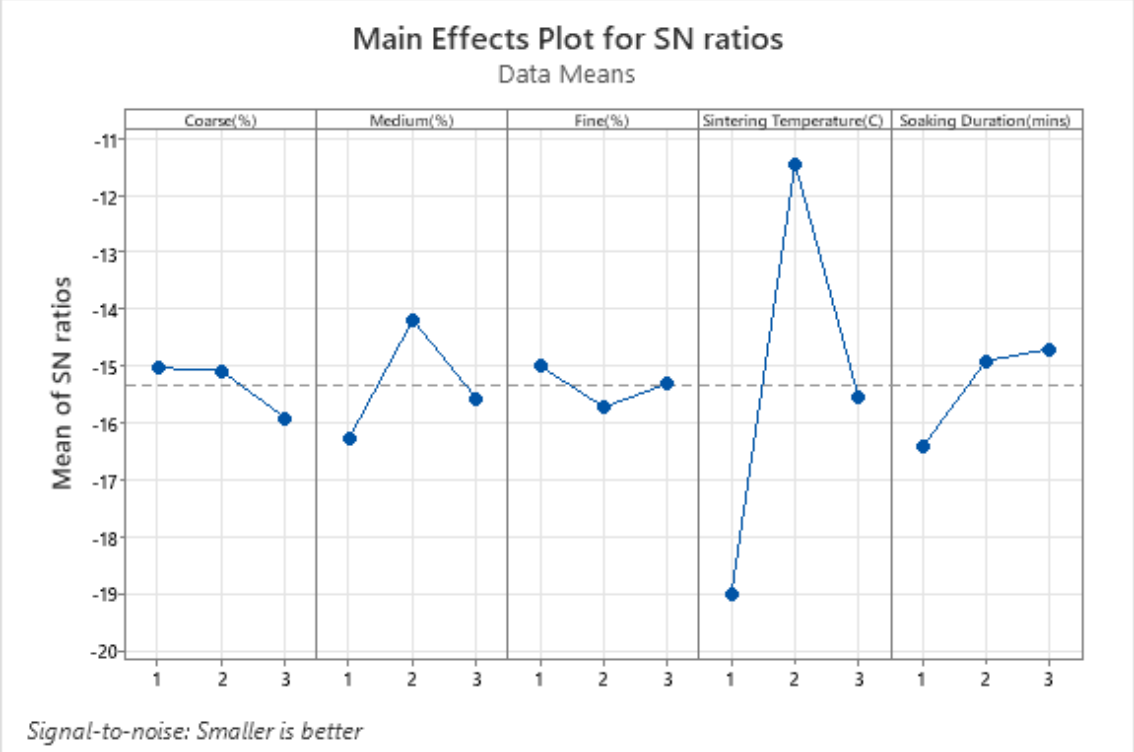

Fig 34: Main effects plot for S/N ratios

Confirmatory test: The confirmatory test was carried out under the optimum conditions to validate the optimization method. A pressed sample was prepared using the optimized coarse, medium, and fine size fractions and it was sintered at a temperature of 1350^0C with a soaking duration of 60 mins. The apparent porosity value of the sintered sample prepared under optimized conditions was found to be **2.26%** which was lower than the minimum porosity value obtained in the above response table.

Analysis of Variance (ANOVA): The percentage contribution of each input parameter towards the response variable was determined using the analysis of variance (ANOVA). In the ANOVA the F-values and P-values are mainly used to determine the contribution of each factor in the optimization. A parameter with a P-value less than 0.05 is considered significant [41].

Table 13: Analysis of Variance for AP

Source	DF	Seq SS	Adj SS	Adj MS	F	P	Contribution%
Coarse %	2	4.422	4.422	2.211	0.48	0.626	1.17
Medium %	2	80.249	60.249	10.125	2.21	0.037	21.03
Fine %	2	2.352	2.352	1.176	0.26	0.777	0.62
Sint Temp	2	179.257	179.257	129.629	28.23	0.000	47.73
Soaking time	2	68.940	15.940	7.970	1.74	0.208	18.35
Residual Error	16	42.464	37.464	4.591			11.30
Total	26	375.685					

The results obtained from Table 13 concluded Sintering Temperature, Medium% and Soaking Time as the most significant factors. The percentage contribution of each parameter was calculated using the Seq SS values obtained from the ANOVA table. The results revealed Sintering Temperature as the most significant parameter in response variable with contribution of 47.7% [42].

The mathematical relationship between the output parameter (Apparent Porosity) and the input parameters as predicted by the model is given as:

Apparent Porosity = 10.23 + 0.243Coarse% - 0.054Medium% - 0.042Fine% - 1.483 Sintering Temperature – 0.584 Soaking Time

3-D response surface plots were determined to study the combined effect of any two parameters on the response variable (AP) by keeping the other parameters constant. In this way several response surface plots were obtained from which the interaction effects can be evaluated.

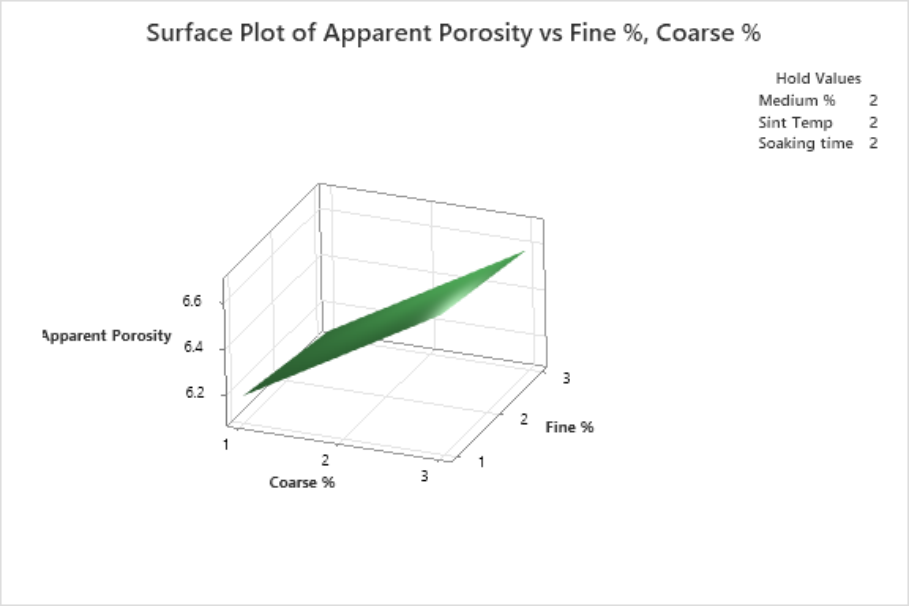

Fig 35: Interaction effects of Coarse and Fine size fraction on AP

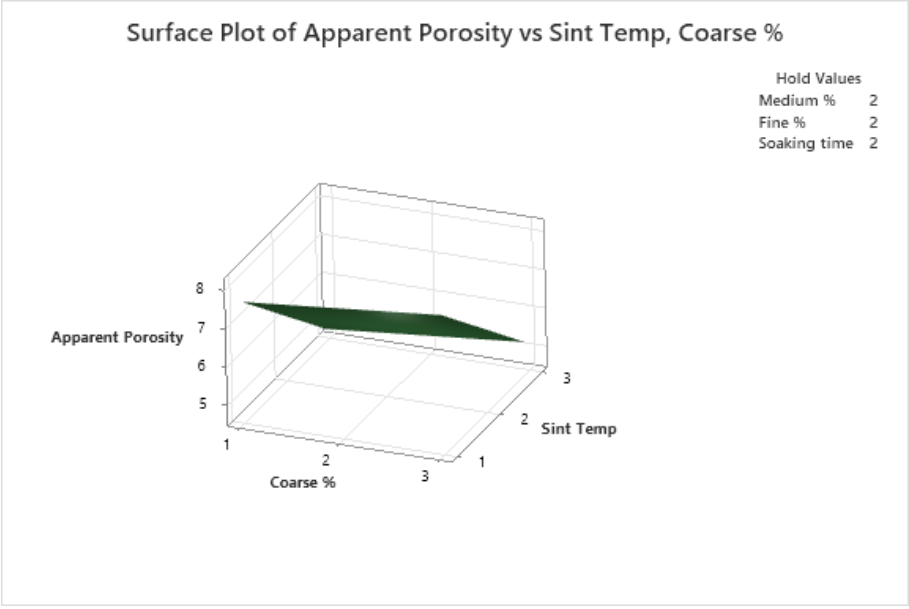

Fig 36: Interaction effects of Coarse size fraction and Sintering Temperature on AP

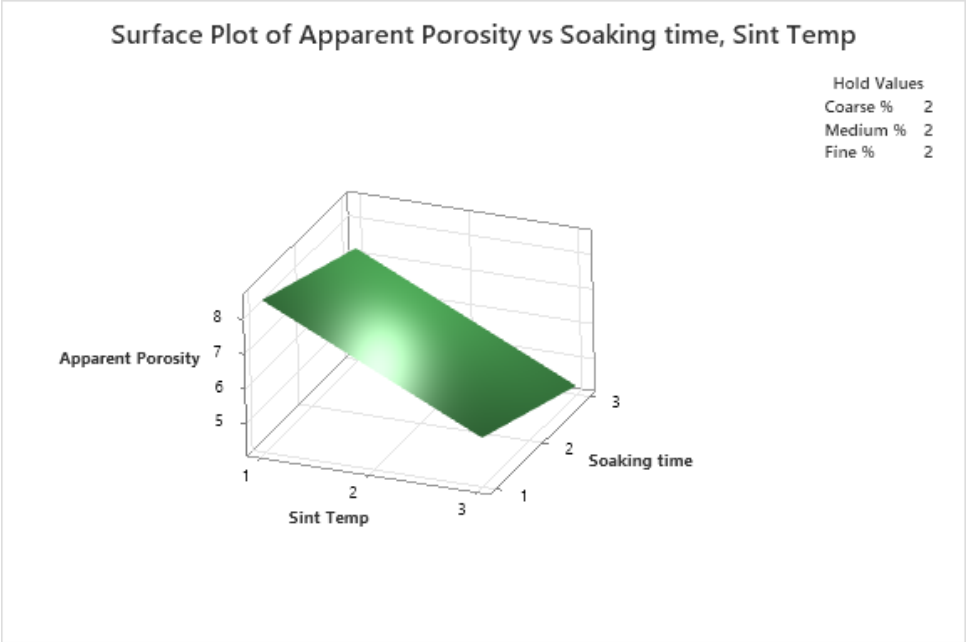

Fig 37: Interaction effects of Soaking Time and Sintering Temperature on AP

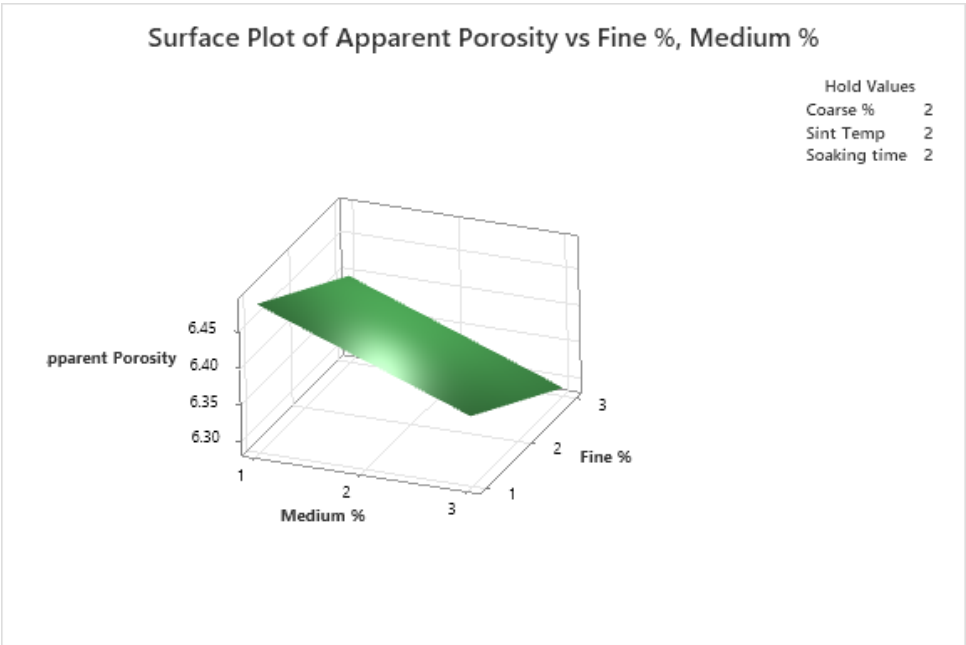

Fig 38: Interaction effects of Medium and Fine size fraction on AP

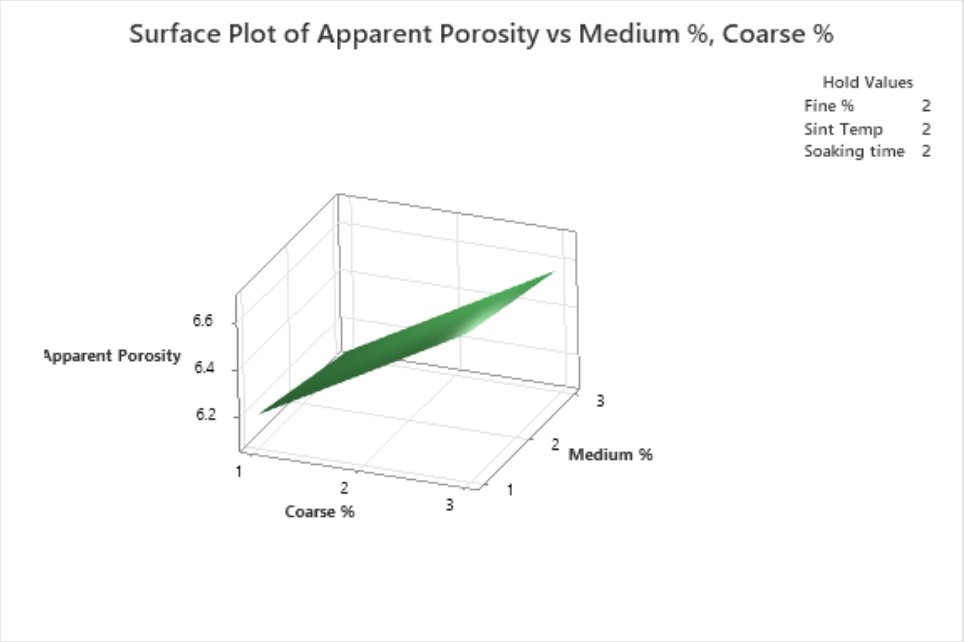

Fig 39: Interaction effects of Coarse and Medium size fractions on AP

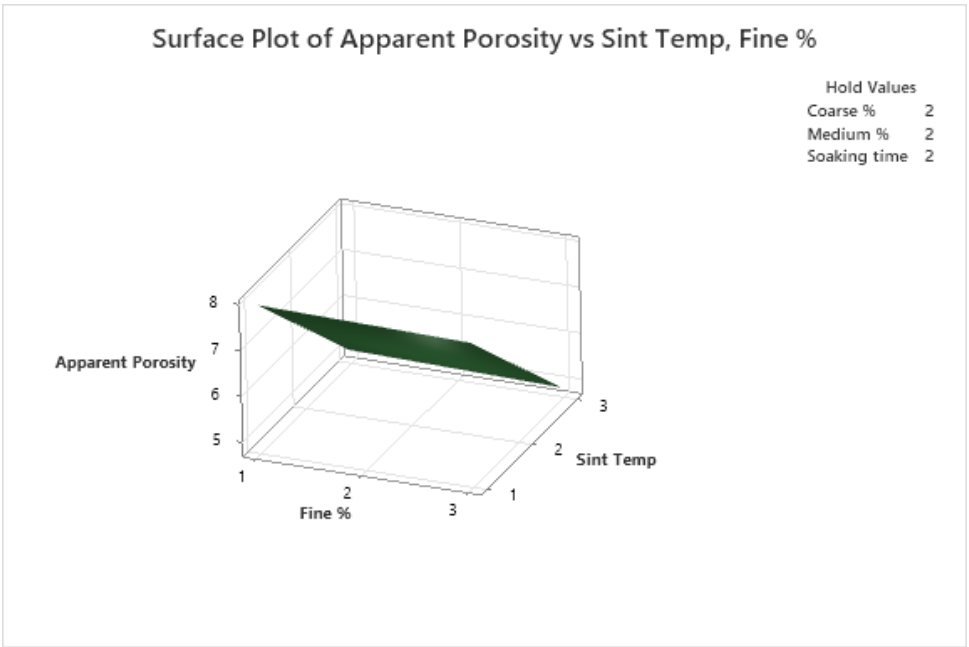

Fig 40: Interaction effects of Sintering Temperature and Fine size fraction on AP

CHAPTER-8
OVERALL CONCLUSION AND FUTURE SCOPE OF WORK

Overall Conclusion:

The entire experimental work involved various methods and techniques to study the effect of different factors on the porosity (and hence mechanical property) of refractories. The results and the conclusions obtained in various steps are summarized below:

- The refractory material chosen for the experiment was fireclay. The fireclay grog was screened into different size fractions (coarse, medium and fine) and then pressed samples were prepared using different batch compositions.
- The dimensions of the samples were noted down and then the samples were fired at different temperatures: 1250^0C, 1350^0C, 1450^0C
- A reduction in volume (volume shrinkage) was observed in all the samples which supported the phenomenon of sintering.
- The samples were sintered at different soaking periods to study the effect of soaking duration on the apparent porosity.
- The apparent porosity values of the sintered samples were measured using 'Boiling Water Method'
- From the values of volume shrinkage and apparent porosity at different temperatures and soaking durations, graphs were plotted to observe the variation of volume shrinkage and porosity with temperature and soaking time.
- The volume shrinkage increased with increase in sintering temperature, however in case of soaking time, volume shrinkage showed an initial increase followed by a slight decrease in value.
- The apparent porosity decreased with increase in sintering temperature. With increase in soaking time minimum apparent porosity value was observed at a soaking duration of 45 min followed by a slight increase.
- The above observations suggested an inverse relation between apparent porosity and volume shrinkage.
- XRD analysis of the sintered fireclay samples revealed higher concentration of mullite phases with increase in sintering temperature. This observation concluded the greater extent of sintering with increase in temperature.
- The SEM images of the sintered fireclay samples revealed decrease in void spaces and improved particle morphology. These images support the improvement in strength of the sintered material due to removal of voids and densification.

- Fuller distribution method was used to select the suitable batch composition to produce the most compact samples. From the different distribution curves, the distribution curve for sample A (45:10:45) showed the least deviation from the ideal Fuller curve and was thus considered as the optimized batch composition. The observation was also validated by confirmatory test
- A correlation between the two parameters of Fuller distribution viz, Coefficient of Uniformity (CU) and Root Mean Square Deviation (RMSD) was established. The results suggested an inverse exponential relationship between the two parameters.
- Taguchi method of optimization was applied by considering coarse %, medium %, fine %, sintering temperature and soaking duration as the input parameters. A 5 factor 3 level design of experiment was performed. The set of optimized parameters predicted by Taguchi method were: **$Coarse_1$ (35-45%), $Medium_2$ (10-20%), $Fine_1$ (35-45%), Sintering $Temperature_2$ (1350^{0}C), $Soaking\ time_3$** (60mins). A minimum porosity of **2.26%** was obtained for the fireclay sample prepared under the optimized conditions.
- Analysis of Variance (ANOVA) table concluded Sintering Temperature, Medium % and Soaking Temperature as the significant factors for the response.
- The optimized batch composition predicted by Taguchi method was in line with the results predicted by Fuller distribution.

Through this optimization minimum porosity was achieved at an intermediate sintering temperature of 1350^{0}C and a soaking duration of 60mins which can lead to reduction in overall cost of the refractory. The Taguchi method was quite successful in providing an idea regarding the optimization of mechanical properties of refractories by using porosity as a response.

Future Scope of Work:

- In this experimental work, optimization of the mechanical property of refractories was done by using apparent porosity as a response variable. However, for more appropriate and satisfactory results mechanical properties like Cold Crushing Strength (CCS), Modulus of Rupture (MOR) can directly be used as a response to get better results.
- In this study, Fuller distribution was used to determine the best suitable batch composition to produce the most compact sample. However, the best selected batch

composition also showed certain deviation from the ideal Fuller curve which can further be minimized by adding some percentages of fine size fractions in the mixture.

- In this study, Taguchi method was applied for optimization however modelling tools like Artificial Neural Networking (ANN) can also be applied to predict the response value more accurately on inserting the input parameters.
- In this study apart from the selected parameters, other parameters like pressing load, percentage of water added, amount of binder added etc. can also significantly affect the properties and their effect can also be considered for future studies.

References:

1. *Refractory Technology Fundamentals and Applications*. (n.d.).

2. Katsavou, I. D., Krokida, M. K., & Ziomas, I. C. (2011). Effect of production conditions on structural properties of refractory materials. *Materials Research Innovations*, *15*(1), 47–52. https://doi.org/10.1179/143307511X12922272563824

3. Obinich, N., & Briggs, T. A. (n.d.). Mathematical Modeling of The Refractory Properties for Kaolinite Clays in Nigeria. *IOSR Journal of Mechanical and Civil Engineering (IOSR-JMCE) e-ISSN*, *13*(6), 125–132. https://doi.org/10.9790/1684-130602125132

4. Deneen, M. A., & Gross, A. C. (2010). Refractory materials: The global market, the global industry. *Business Economics*. https://doi.org/10.1057/be.2010.30

5. *Ministry of Steel Government of India*. (n.d.).

6. FRANCL, J., & KINGERY, W. D. (1954). Thermal Conductivity: IX, Experimental Investigation of Effect of Porosity on Thermal Conductivity. *Journal of the American Ceramic Society*, *37*(2), 99–107. https://doi.org/10.1111/j.1551-2916.1954.tb20108.x

7. Kurgan, N. (2014). Effect of porosity and density on the mechanical and microstructural properties of sintered 316L stainless steel implant materials. *Materials and Design*, *55*, 235–241. https://doi.org/10.1016/j.matdes.2013.09.058

8. Shalabi, M. E. H., Elngar, M. A. G., Mohamed, F. M., El-Bohy, S. A. H., Sharaby, C. M., El-Menshawi, M., & Shalabi, H. (2009). *Factors Affected the Performance of the Fire Clay Refractory Bricks*. *journal gornictwo I Geoinzynieria* (Vol. 4). Retrieved from https://www.researchgate.net/publication/268575397

9. Vieira, C. M. F., & Monteiro, S. N. (2006). Effect of the Particle Size of the Grog on the Properties and Microstructure of Bricks. *Materials Science Forum*, *530–531*, 438–443. https://doi.org/10.4028/www.scientific.net/msf.530-531.438

10. Adamu, H. A., Samuel, B. O., Joseph, A., Okon, S. S., & Kirim, I. I. (2023). Production and optimization of the refractory properties of blended Nigerian clay for high-temperature application; a non-stochastic optimization approach. *Functional Composites and Structures*, *5*(2). https://doi.org/10.1088/2631-6331/acc9fb

11. Sutcu, M., Ozturk, S., Yalamac, E., & Gencel, O. (2016). Effect of olive mill waste addition on the properties of porous fired clay bricks using Taguchi method. *Journal of Environmental Management*, *181*, 185–192. https://doi.org/10.1016/j.jenvman.2016.06.023

12. Sarkar, B. K., Kumar, N., Dey, R., & Das, G. C. (2018). Optimization of Quenching Parameters for the Reduction of Titaniferous Magnetite Ore by Lean Grade Coal Using the Taguchi Method and Its Isothermal Kinetic Study. *Metallurgical and Materials Transactions B: Process Metallurgy and Materials Processing Science*, *49*(4), 1822–1833. https://doi.org/10.1007/s11663-018-1283-y

13. Dana, K., Sinhamahapatra, S., Tripathi, H. S., & Ghosh, A. (2014). Refractories of Alumina-Silica System. *Transactions of the Indian Ceramic Society*. I N S I O Scientific Books and Periodicals. https://doi.org/10.1080/0371750X.2014.905265

14. Chaudhuri, S. P., & Bhaumik, B. K. (1997). *Constitution and properties of ceramized fireclay refractories: I. Constitution*. *Bull. Mater. Sci* (Vol. 20).

15. Chaudhuri, S. P., & Bhaumik, B. K. (1997). *Constitution and properties of ceramized fireclay refractories: II. Properties*. *Bull. Mater. Sci* (Vol. 20).

16. Rahman, M. F. (2012). *Properties of fire clay after dressing and the effect of grog*. *Proceedings of the Global Engineering*.

17. Czechowski, J., Podwórny, J., Czechowski, J., Gerle, A., Podwórny, J., & Dahlem, E. (n.d.). *Investigation of the Testing Parameters Influencing the Cold Crushing Strenght Testing Results of Refractory Materials Technology Trends Investigation of the Testing Parameters Infl uencing the Cold Crushing Strength Testing Results of Refractory Materials*. Retrieved from https://www.researchgate.net/publication/280715236

18. Mohamed Ariff, A. H., Mohamad Najib, M. A., Mohd Tahir, S., As'Arry, A., & Mazlan, N. (2021). Effect of sintering temperature on the properties of porous Al2O3-10 wt% RHA/10 wt% Al composite. *Advances in Materials and Processing Technologies*, *7*(3), 417–428. https://doi.org/10.1080/2374068X.2020.1785204

19. Karaman, S., Ersahin, S., & Gunal, H. (2006). *Firing temperature and firing time influence on mechanical and physical properties of clay bricks*. *Journal of Scientific & Industrial Research* (Vol. 65).

20. Amkpa, J. A., Badarulzaman, N. A., & Aramjat, A. B. (2016). Influence of Sintering Temperatures on Physico-Mechanical Properties and Microstructure of Refractory Fireclay Bricks. *International Journal of Engineering and Technology*, *8*(6), 2588–2593. https://doi.org/10.21817/ijet/2016/v8i6/160806214

21. Najim, M. M., & Yousif, A. (n.d.). *53 (2F), 2020: 49-64 EFFECT OF SINTERING AND CORDIERITE ADDITIVES ON THE PHYSICAL AND MECHANICAL PROPERTIES OF MULLITE BASED CERAMICS PREPARED FROM IRAQI RAW MATERIALS EFFECT OF SINTERING AND CORDIERITE ADDITIVES ON THE PHYSICAL AND MECHANICAL PROPERTIES OF MULLITE BASED CERAMICS PREPARED FROM IRAQI RAW MATERIALS*. Retrieved from https://www.researchgate.net/publication/349710829

22. Okafor, G., Iyasara, A. C., Stan, E. C., Geoffrey, O., Joseph, M., Patrick, N. N., & Benjamin, N. (2016). Influence of Grog Size on the Performance of NSU Clay-Based Dense Refractory Bricks. *American Journal of Materials Science and Engineering*, *4*(1), 7–12. https://doi.org/10.12691/ajmse-4-1-2

23. Schafföner, S., Dietze, C., Möhmel, S., Fruhstorfer, J., & Aneziris, C. G. (2017). Refractories containing fused and sintered alumina aggregates: Investigations on processing, particle size distribution and particle morphology. *Ceramics International*, *43*(5), 4252–4262. https://doi.org/10.1016/j.ceramint.2016.12.067

24. Prasad, T. V. (1970). Effect of forming pressure on the physical properties and high temperature load bearing characteristics of basic refractories. *Transactions of the Indian Ceramic Society*, *29*(1), 11–18. https://doi.org/10.1080/0371750X.1970.10855715

25. Schafföner, S., Fruhstorfer, J., Ludwig, S., & Aneziris, C. G. (2018). Cyclic cold isostatic pressing and improved particle packing of coarse grained oxide ceramics for refractory applications. *Ceramics International*, *44*(8), 9027–9036. https://doi.org/10.1016/j.ceramint.2018.02.106

26. Zou, Y., Huang, A., Gu, H., Zhang, M., & Lian, P. (2016). Effects of particle distribution of matrix on microstructure and slag resistance of lightweight Al2O3-MgO castables. *Ceramics International*, *42*(1), 1964–1972. https://doi.org/10.1016/j.ceramint.2015.09.167

27. Naito, M., Hayakawa, O., Nakahira, K., Mori, H., & Tsubaki, J. (1998). *Effect of particle shape on the particle size distribution measured with commercial equipment*. *Powder Technology* (Vol. 100).

28. Kalpakli, Y. K. (2008). *Effects of particle size distribution on the refractory properties and corrosion ultra-low cement castables*.

29. *Chapter 6B Study of Fuller Curve Method and Direct Reduction Behavior*. (n.d.).

30. Guo, Z.-Q., & Zhang, H. (n.d.). *The Optimization of the Microstructure and Phase Assemblage of High Chromia Refractories*.

31. Doroganov, V. A., Doroganov, E. A., Bel'maz, N. S., Timoshenko, K. V., Trepalina, Y. N., Peretokina, N. A., … Evtushenko, E. I. (2009). Development and study of Composite refractory materials based on modified dispersed systems. *Refractories and Industrial Ceramics*, *50*(6), 431–437. https://doi.org/10.1007/s11148-010-9232-6

32. Jastrzębska, I., & Szczerba, J. (2024, April 1). Design, Manufacturing and Properties of Refractory Materials. *Materials*. Multidisciplinary Digital Publishing Institute (MDPI). https://doi.org/10.3390/ma17071673

33. Raheem, Z. (2019). Standard Test Methods for Apparent Porosity, Water Absorption, Apparent Specific Gravity, and Bulk Density of Burned Refractory Brick and Shapes by Boiling Water 1 Some of the authors of this publication are also working on these related projects: photocatalytic View project photocatalytic View project. https://doi.org/10.1520/C0020-00R10

34. Gong, C., Zhang, J., Wang, S., & Lu, L. (2015). Effect of aggregate gradation with fuller distribution on properties of sulphoaluminate cement concrete. *Journal Wuhan University of Technology, Materials Science Edition*, *30*(5), 1029–1035. https://doi.org/10.1007/s11595-015-1268-5

35. Shado, A. S., Oj, A., & Ca, U. (2018). *The Effect of Grog Sizing on the Performance of Ire Ekiti Fire Clay Refractory Bricks*. Retrieved from https://www.researchgate.net/publication/324521693

36. Lomertwala, H. M., Njoroge, P. W., Opiyo, S. A., & Ptoton, B. M. (2019). Characterization of Clays from selected sites for Refractory Application. *International Journal of Scientific and Research Publications (IJSRP)*, *9*(11), p9581. https://doi.org/10.29322/ijsrp.9.11.2019.p9581

37. Chen, J., Zhao, H., Zhang, H., Li, Z., & Zhang, J. (2018). Sintering and microstructural characterization of calcium alumino-titanate-bauxite-SiC composite refractories. *Ceramics International*, *44*(9), 10934–10939. https://doi.org/10.1016/j.ceramint.2018.03.157

38. Job Ajala, A., Badarulzaman, N. A., & Aramjat, A. B. (2017). Impact of sintering temperatures on microstructure, porosity and mechanical strength of refractory brick. In *Materials Science Forum* (Vol. 888 MSF, pp. 66–70). Trans Tech Publications Ltd. https://doi.org/10.4028/www.scientific.net/MSF.888.66

39. Xiang, J., Liu, L., Cui, X., He, Y., Zheng, G., & Shi, C. (2019). Effect of Fuller-fine sand on rheological, drying shrinkage, and microstructural properties of metakaolin-based geopolymer grouting materials. *Cement and Concrete Composites*, *104*. https://doi.org/10.1016/j.cemconcomp.2019.103381

40. Ghani, J. A., Choudhury, I. A., & Hassan, H. H. (2004). Application of Taguchi method in the optimization of end milling parameters. *Journal of Materials Processing Technology*, *145*(1), 84–92. https://doi.org/10.1016/S0924-0136(03)00865-3

41. Yang, W. H., & Tarng, Y. S. (1998). *Design optimization of cutting parameters for turning operations based on the Taguchi method*. *Journal of Materials Processing Technology* (Vol. 84).

42. Mustapha, A. N., Zhang, Y., Zhang, Z., Ding, Y., Yuan, Q., & Li, Y. (2021). Taguchi and ANOVA analysis for the optimization of the microencapsulation of a volatile phase change material. *Journal of Materials Research and Technology*, *11*, 667–680. https://doi.org/10.1016/j.jmrt.2021.01.025